

UNIVERSITY OF TARTU

FACULTY OF SCIENCE AND TECHNOLOGY

Institute of Physics

Paul Martin Kull

Radially anisotropic wormholes in $f(R, T)$ gravity

Bachelor's thesis (6 ECTS)

Physics, Chemistry and Material Science program, Physics curriculum

Supervisor:

João Luís Rosa, PhD

Tartu 2022

Abstract

Radially anisotropic wormholes in $f(R, T)$ gravity

In this thesis, stable traversable wormhole models are developed in the geometric and scalar-tensor representations of $f(R, T)$ gravity, using the thin-shell formalism to match the wormhole spacetime with an exterior Kottler spacetime in an attempt to satisfy the null energy condition everywhere. After deriving the junction conditions for the particular forms of the theory used in this thesis, one finds that in the geometric case, the radius r_Σ of the thin-shell is not restricted to single values for some combinations of the particular form of $f(R, T)$, the shape and redshift functions $b(r)$ and $\zeta(r)$, and the throat radius r_0 . This allows one to choose r_Σ and the exterior cosmological constant Λ such that the weak energy condition can also be satisfied everywhere. In the scalar-tensor case, r_Σ is instead restricted to a finite number of values for any given initial r_0 , $b(r)$, $\zeta(r)$ and the scalar field interaction potential $V(\varphi, \psi)$, meaning that the value of r_Σ must be calculated before one can attempt a matching. For this case, an algorithm is employed that attempts the matching for various combinations of these initial parameters, but no combinations are found that satisfy the wormhole null energy condition within r_Σ .

CERCS: P190 - Mathematical and general theoretical physics, classical mechanics, quantum mechanics, relativity, gravitation, statistical physics, thermodynamics.

Keywords: Modified gravity, wormholes, thin-shell formalism.

Radiaalselt anisotroopsed ussiaugud $f(R, T)$ gravitatsiooniteoorias

Selles töös luuakse mudelid stabiilsete ning läbitavate ussiaukude jaoks $f(R, T)$ gravitatsiooni-teooria geomeetrilise ning skalaar-tensor esituste raames. Isotroopse energiatingimuse kõikjal rahuldamiseks kasutatakse õhukese kihi formalismi, kus ussiaugu aegruum sobitatakse sellest väljaspool oleva Kottleri aegruumiga. Peale selles töös kasutatavate pidevustingimuste tule-tamist leitakse, et geomeetrilises esituses ei oma õhukese kihi raadius r_Σ lõplikku arvu lubatud väärtusi, kui valida kindlad kujud funktsiooni $f(R, T)$, kuju- ja punanihkefunktsioonide $b(r)$ ja $\zeta(r)$, ning ussiaugu kõri raadiuse r_0 jaoks. See võimaldab valida r_Σ ning välise kosmoloogilise konstandi Λ väärtused selliselt, et ka nõrka energiatingimust on võimalik kõikjal rahuldada. Skalaar-tensor esituses võib r_Σ omada vaid lõplikku arvu väärtusi iga algse r_0 , $b(r)$, $\zeta(r)$ ning skalaarväljade omavahelise potentsiaali $V(\varphi, \psi)$ puhul, mis tähendab, et enne sobitamist on vaja arvutada r_Σ väärtus. Selleks kasutatakse algoritmi, mille abil viiakse läbi sobitamine erinevate eelmainitud algparameetrite jaoks, kuid ei tuvastata ühtegi parameetrite kombinatsiooni, kus ussiaugu isotroopne energiatingimus on r_Σ sees rahuldatud.

CERCS: P190 - Matemaatiline ja üldine teoreetiline füüsika, klassikaline mehaanika, kvant-mehaanika, relatiivsus, gravitatsioon, statistiline füüsika, termodünaamika.

Märksõnad: Modifitseeritud gravitatsioon, ussiaugud, õhukese kihi formalism.

Contents

Introduction	5
Glossary	7
1 Theoretical introduction	10
1.1 Wormholes	10
1.2 $f(R,T)$ gravity	12
1.2.1 Geometric representation	12
1.2.2 Scalar-tensor representation	13
1.3 Thin-shell formalism and junction conditions	17
1.3.1 Geometric representation	19
1.3.2 Scalar-tensor representation	20
2 Wormhole solutions	23
2.1 Geometric representation	24
2.1.1 Matter quantities	24
2.1.2 Spacetime matching	25
2.2 Scalar-tensor representation	29
2.2.1 Matter quantities	29
2.2.2 Spacetime matching	30
Conclusions	33
Acknowledgements	34
Bibliography	34
A <i>Wolfram Mathematica</i> code	39
B Scalar-tensor matching data	50
C Derivation for the explicit form of $\Theta_{\mu\nu}$	51
Non-exclusive licence to reproduce the thesis and make the thesis public	52

Introduction

Wormholes are hypothetical objects that connect two points in spacetime – like a tunnel, to provide a simple analogy. They were initially proposed as a prediction of Einstein’s theory of general relativity (GR), more specifically as a possible consequence of the Schwarzschild solution. However, these ”Schwarzschild wormholes” are not traversable. Unlike a black hole, a (traversable) wormhole does not possess an event horizon or a singularity. Instead, it presents a point of minimal radius, referred to as ”the throat” in this thesis. [1]

In GR, stable traversable wormholes violate the *null energy condition* (NEC) at the throat, implying that they require exotic matter to exist. As such matter has currently not been observed in astrophysical systems, it is useful and more physically relevant to consider theories of gravity where modifications in the gravitational sector may compensate for the need for it. One well-studied extension to GR is $f(R)$ theory, where the Ricci scalar R in the Einstein-Hilbert action of GR is replaced by a function of R . This theory has proven successful in a wide variety of cosmological scenarios [2, 3, 4, 5, 6], but some specific models have been ruled out by Solar System tests [7, 8] or the presence of instabilities [9]. Due to these issues, further extensions may be considered. One example is $f(R, T)$ theory, where the function of R in the action of the theory is replaced by a function of both R and the trace of the stress-energy tensor T . This theory has also proven useful in various astrophysical contexts [10, 11, 12], but many of its nuances currently remain unstudied.

Developing wormhole models that satisfy the NEC everywhere is generally a difficult task that strongly depends on the assumptions of the given theory and wormhole system. For this reason, it is practical to use alternative approaches to satisfy the NEC everywhere. One such approach is the *thin-shell formalism*, which only requires the wormhole model to satisfy the NEC in a small region but places additional restrictions on the model, known as *junction conditions*.

As stated above, $f(R)$ theory has been extensively studied in many contexts. For example, it has proven suitable for explaining the accelerating expansion of the Universe [2, 3] and has provided a substitute for dark matter [4, 5, 6]. However, some models have been ruled out by weak-field limit tests [7, 8] and matter instabilities [9]. Many similar topics have also been explored in $f(R, T)$ theory [10, 11, 12], though sometimes with only limited success in satisfying observational data [13].

Many different theories of modified gravity have been used to consider traversable wormhole models with varying degrees of success. For example, one case of an $f(R)$ theory-based wormhole model only satisfied the transverse NEC inequality [14]. In addition, models have been developed within hybrid metric-Palatini theory, using the thin-shell formalism [15], and in GR [16], where the latter only violates the NEC near the Planck scale. Wormhole models have also been considered within $f(R, T)$ theory [17, 18], but not by using its scalar-tensor representation or the thin-shell formalism. The junction conditions of $f(R, T)$ theory, which will be required for the wormhole models in this thesis, have been derived for the case of a perfect fluid [19], and the particular cases considered in this thesis are presented in Section 1.3. Finally, wormhole models that satisfy the NEC everywhere without the thin-shell formalism have been proven to exist in some theories of gravity, such as Gauss-Bonnet [20], beyond Horndeski [21], $f(R)$ [22], and $f(R, T)$ theory with isotropic pressure [17].

This thesis aims to develop new and physically relevant traversable wormhole models using the $f(R, T)$ theory of gravity and thus provide new insights into the physics of the theory and of wormholes themselves. To this end, the thin-shell formalism will be used to create a model that satisfies the NEC everywhere. The task of doing so without the thin-shell formalism is left as a topic of future research. In addition, both the geometric and scalar-tensor representations of $f(R, T)$ gravity will be used to create two different wormhole models to explore these representations' respective (dis)advantages. The main body of this thesis is organised into two chapters: first, Chapter 1 will provide an overview of wormholes, $f(R, T)$ theory, including the particular cases of it used in this thesis, and the thin-shell formalism, and derive the junction conditions used in the following chapter. Second, Chapter 2 will focus on developing particular wormhole models by deriving the explicit junction conditions and expressions for the NEC and attempting to find cases where they are satisfied. Where relevant, the geometric and scalar-tensor representations will have separate (sub)sections dedicated to them.

Glossary

Note that, unless specified otherwise, this glossary is based on [23].

Coordinates and units

As all spacetimes studied in this thesis possess spherical symmetry, all calculations will be performed using the spherical coordinates $x^\mu = (t, r, \theta, \phi)$. In addition, geometrised units, where the speed of light and Newton's gravitational constant are set to unity, i.e. $c = G = 1$, will be used subsequently. If desired, one may always convert any results into SI units by reintroducing the constants c and G as needed using dimensional analysis.

The **Einstein summation convention** is a concise way of writing tensor equations where any indices that appear "paired," such that they have the same value, with one being co- and the other contravariant, are called summation indices (and are summed over), and any unpaired indices are free indices. The summation sign for a given summation index is also omitted, e.g. the scalar product of two vectors a and b in Cartesian coordinates can be written as

$$a \cdot b = \sum_i a_i b^i \equiv a_i b^i, \quad (1)$$

where a_i and b_i are the components of the vectors. For example, in this case, i is a summation index, and there are no free indices.

The choice of a **sign convention** arises from the need to write the time and spatial coordinates of spacetime with opposing signs. As such, one may choose to have either a negative time coordinate with positive spatial coordinates or vice versa. Both choices are equivalent, but the sign convention with a negative time coordinate will be used in this thesis.

The **metric** $g_{\mu\nu}$ is a second rank symmetric tensor that describes the geometry of a given spacetime. The metric does not need to be constant throughout spacetime. In this thesis, the metric and any other tensor will be referred to in terms of its components, omitting the relevant

basis vectors. Furthermore, the inverse metric $g^{\mu\nu}$ and the metric determinant g are defined as

$$g^{\mu\nu} \equiv (g_{\mu\nu})^{-1}, \quad g \equiv \det(g_{\mu\nu}). \quad (2)$$

The **Christoffel symbols** (of the second kind) $\Gamma^\rho_{\mu\nu}$ are the Levi-Civita connection coefficients, which determine how an orthonormal basis changes from point to point on a manifold. The Christoffel symbols can be stated in terms of the metric as

$$\Gamma^\rho_{\mu\nu} = \frac{1}{2}g^{\rho\alpha}(\partial_\nu g_{\alpha\mu} + \partial_\mu g_{\alpha\nu} - \partial_\alpha g_{\mu\nu}). \quad (3)$$

The **Riemann tensor** $R^\rho_{\sigma\mu\nu}$ is a 4th rank tensor that expresses the curvature of spacetime. It is usually stated in terms of the Christoffel symbols as

$$R^\rho_{\sigma\mu\nu} = \partial_\mu \Gamma^\rho_{\nu\sigma} - \partial_\nu \Gamma^\rho_{\mu\sigma} + \Gamma^\rho_{\mu\lambda} \Gamma^\lambda_{\nu\sigma} - \Gamma^\rho_{\nu\lambda} \Gamma^\lambda_{\mu\sigma}. \quad (4)$$

The **Ricci tensor** $R_{\mu\nu}$ may be defined as a contraction of the Riemann tensor by the first and third indices:

$$R_{\mu\nu} = R^\rho_{\mu\rho\nu}. \quad (5)$$

The **Ricci scalar** R , also known as the scalar curvature, is the contraction of the Ricci tensor with the metric:

$$R \equiv g^{\mu\nu} R_{\mu\nu} = R^\mu_{\mu}. \quad (6)$$

The **covariant derivative** ∇_μ , where μ represents the spacetime coordinate x^μ with respect to which the derivative is taken, is a generalisation of the partial derivative that accounts for the curvature of spacetime in describing infinitesimal changes of vectors and tensors. In general, the covariant derivative of a tensor field A with p contravariant and q covariant indices is

$$\begin{aligned} \nabla_\mu A^{\underbrace{\kappa\lambda\ldots}_p \underbrace{\alpha\beta\ldots}_q} &= \partial_\mu A^{\kappa\lambda\ldots}_{\alpha\beta\ldots} + \underbrace{\Gamma^\kappa_{\sigma\mu} A^{\sigma\lambda\ldots}_{\alpha\beta\ldots} + \Gamma^\lambda_{\sigma\mu} A^{\kappa\sigma\ldots}_{\alpha\beta\ldots} + \ldots}_{p \text{ of these terms in total}} \\ &\quad - \underbrace{\Gamma^\sigma_{\alpha\mu} A^{\kappa\lambda\ldots}_{\sigma\beta\ldots} - \Gamma^\sigma_{\beta\mu} A^{\kappa\lambda\ldots}_{\alpha\sigma\ldots} - \ldots}_{q \text{ of these terms in total}}, \end{aligned} \quad (7)$$

where $\partial_\mu \equiv \frac{\partial}{\partial x^\mu}$ is a concise way of writing the partial derivative with respect to x^μ . Note that the Christoffel symbols are generally functions of the metric and therefore the covariant derivative is as well. As such, in this thesis any covariant derivative will be with respect to the

wormhole metric unless stated otherwise. A special case of the above expression is for a scalar field λ , where the covariant derivative is equivalent to the partial derivative:

$$\nabla_\mu \lambda = \partial_\mu \lambda. \quad (8)$$

The **stress-energy tensor** $T_{\mu\nu}$ is a 2nd rank tensor that describes the properties of a given matter distribution. The trace of this tensor is defined as $T \equiv g^{\mu\nu} T_{\mu\nu} = T^\mu{}_\mu$. In this thesis, the stress-energy tensor is given with the first index raised, so $T^\mu{}_\nu = g^{\mu\alpha} T_{\alpha\nu}$, and in a comoving frame of reference, in which case its only nontrivial components are on the main diagonal.

The **energy conditions** are sets of inequalities formulated to ensure that no observer will encounter negative average energy or mass density within a given matter distribution, ensuring consistency with observations. Generally, the energy conditions are defined in terms of the stress-energy tensor of the observed matter. In the case of a radially anisotropic perfect fluid, the stress-energy tensor is given by

$$T^\mu{}_\nu = \begin{pmatrix} -\rho & 0 & 0 & 0 \\ 0 & p_r & 0 & 0 \\ 0 & 0 & p_t & 0 \\ 0 & 0 & 0 & p_t \end{pmatrix}, \quad (9)$$

where ρ is the energy density of the fluid and p_r, p_t are the radial and transverse pressures in the fluid, respectively. In this case, the energy conditions are as follows: (see [23], pp. 30-31 and [24], pp. 115-116)

$$\text{Null Energy Condition (NEC): } \rho + p_r \geq 0, \rho + p_t \geq 0, \quad (10)$$

$$\text{Weak Energy Condition (WEC): } \rho + p_r \geq 0, \rho + p_t \geq 0, \rho \geq 0, \quad (11)$$

$$\text{Dominant Energy Condition (DEC): } \rho \geq |p_r|, \rho \geq |p_t|, \quad (12)$$

$$\text{Strong Energy Condition (SEC): } \rho + p_r \geq 0, \rho + p_t \geq 0, \rho + p_r + 2p_t \geq 0, \quad (13)$$

If a matter distribution violates the NEC, it is considered "exotic." If the NEC is violated, so is every other energy condition. In this thesis, the primary focus will be on attempting to satisfy the NEC and, if possible, the WEC.

1 Theoretical introduction

This chapter aims to provide an overview of the primary theoretical framework of this thesis. Section 1.1 will briefly introduce the geometric and material properties of wormholes and the necessary conditions for a given wormhole to be traversable. Section 1.2 will then present the specifics of the $f(R, T)$ theory of gravity and its field equations in the geometric and scalar-tensor representations. Finally, Section 1.3 will introduce the thin-shell formalism with its associated junction conditions in both representations.

1.1 Wormholes

Before beginning this section, note that it is based on [24], specifically Chapter 11. The geometric properties of a wormhole are encoded in its metric, which in spherical coordinates and with the sign convention chosen for this thesis is given by

$$g_{\mu\nu} = \begin{pmatrix} -e^{\zeta(r)} & 0 & 0 & 0 \\ 0 & \left(1 - \frac{b(r)}{r}\right)^{-1} & 0 & 0 \\ 0 & 0 & r^2 & 0 \\ 0 & 0 & 0 & r^2 \sin^2 \theta \end{pmatrix}. \quad (1.1)$$

This metric contains two functions $\zeta(r)$ and $b(r)$, which require some elaboration:

The **redshift function** $\zeta(r)$ describes the behaviour of gravitational redshift within the spacetime and the **shape function** $b(r)$ describes the shape of the wormhole tunnel. In the case of traversable wormholes, these functions must satisfy the following conditions:

1. To avoid the existence of horizons in the wormhole spacetime, $\zeta(r)$ and $\frac{b(r)}{r}$ must be finite everywhere within it.
2. The shape function must obey the boundary condition $b(r_0) = r_0$, where r_0 is the radius

of the wormhole's throat.

2.1 In addition, r_0 must be larger than the Schwarzschild radius of the wormhole to prevent it from collapsing into a black hole. This means that for any wormhole $r_0 \geq 2M$, where M is the mass of the wormhole.

3. The shape function must also obey the flaring-out condition, which is given by

$$\frac{b(r_0) - b'(r_0)r_0}{[b(r_0)]^2} > 0, \text{ where } b'(r_0) = \left. \frac{db}{dr} \right|_{r=r_0}. \quad (1.2)$$

By also considering that $b(r_0) = r_0$, this condition can be simplified to $b'(r_0) < 1$. The flaring-out condition ensures that at the throat, the radial coordinate of the wormhole spacetime increases in every direction, thereby making the wormhole traversable. This also implies that for a wormhole spacetime $r \in [r_0, \infty)$, unlike in a Schwarzschild or similar spacetime where $r \in [0, \infty)$.

There are many families of functions satisfying these requirements. For this thesis, consider the following particular forms:

$$\zeta(r) = \zeta_0 \left(\frac{r_0}{r} \right)^\alpha, \quad b(r) = r_0 \left(\frac{r_0}{r} \right)^\beta, \quad (1.3)$$

where ζ_0 , α , and β are free parameters. The conditions given above can now be stated in terms of constraints on the values of α and β :

1. $\alpha \geq 0$, otherwise $\zeta(r) \rightarrow \infty$ as $r \rightarrow \infty$,
2. $\beta > -1$, otherwise $\frac{b(r)}{r} \rightarrow \infty$ as $r \rightarrow \infty$. In addition, the flaring-out condition will be violated.

The Ricci scalar of the metric (1.1) with the redshift and shape functions (1.3) is given by

$$R = \frac{[r\zeta'(r) + 4]b'(r) + [3b(r) - 4r]\zeta'(r) + r[b(r) - r][\zeta'(r)^2 + 2\zeta''(r)]}{2r^2}, \quad (1.4)$$

where here and onward in this thesis primes denote derivatives with respect to r .

One must also consider the material properties of the wormhole. In this thesis, it is assumed that the wormhole is static, spherically symmetric, and populated by a perfect fluid with radially

anisotropic pressure, meaning that its stress-energy tensor takes the following form:

$$T^\mu{}_\nu = \begin{pmatrix} -\rho & 0 & 0 & 0 \\ 0 & p_r & 0 & 0 \\ 0 & 0 & p_t & 0 \\ 0 & 0 & 0 & p_t \end{pmatrix}, \quad (1.5)$$

where ρ is the energy density of the fluid and p_r, p_t are the radial and transverse pressures in the fluid, respectively. These will collectively be denoted as the **matter quantities**. The trace of this tensor is

$$T = -\rho + p_r + 2p_t. \quad (1.6)$$

1.2 $f(R, T)$ gravity

1.2.1 Geometric representation

To begin, consider the action of $f(R, T)$ theory:

$$S_{act} = \frac{1}{2\kappa^2} \int_{\Omega} \sqrt{-g} f(R, T) d^4x + \int_{\Omega} \sqrt{-g} \mathcal{L}_m d^4x, \quad (1.7)$$

where $\kappa^2 \equiv \frac{8\pi G}{c^4} = 8\pi$ is the Einstein gravitational constant, Ω is the spacetime manifold on which the metric is defined, and \mathcal{L}_m is the matter Lagrangian. Note that GR is the particular case of $f(R, T)$ theory for which $f(R, T) = R$. By varying this action with respect to the metric, one may obtain the general field equations of $f(R, T)$ gravity, which are

$$\frac{\partial f}{\partial R} R_{\mu\nu} - \frac{1}{2} f(R, T) g_{\mu\nu} + (g_{\mu\nu} \square - \nabla_\mu \nabla_\nu) \frac{\partial f}{\partial R} = 8\pi T_{\mu\nu} - \frac{\partial f}{\partial T} (T_{\mu\nu} + \Theta_{\mu\nu}),^1 \quad (1.8)$$

where $\square \equiv \nabla^\mu \nabla_\mu$ is the covariant d'Alembert operator and $\Theta_{\mu\nu} \equiv g^{\alpha\beta} \frac{\delta T_{\alpha\beta}}{\delta g^{\mu\nu}}$ is a second-rank tensor [10]. Note that $\Theta_{\mu\nu}$ has no explicit physical meaning or connection with observable quantities, as does, for example, the stress-energy tensor. Furthermore, one must first choose a form of the stress-energy tensor to obtain an explicit form of $\Theta_{\mu\nu}$. In the case of a stress-energy

¹See [10] for the full derivation.

tensor given by equation (1.5), $\Theta_{\mu\nu}$ is given by

$$\Theta_{\mu\nu} = -2T_{\mu\nu} + \frac{1}{3}(p_r + 2p_t)g_{\mu\nu}.^2 \quad (1.9)$$

For this thesis, consider the following particular form of the function $f(R, T)$:

$$f(R, T) = R + aT, \quad (1.10)$$

where a is a constant. With this and equation (1.9), the field equations (1.8) can be written as

$$R_{\mu\nu} - \frac{1}{2}(R + aT)g_{\mu\nu} = (8\pi + a)T_{\mu\nu} - \frac{a}{3}(p_r + 2p_t)g_{\mu\nu}, \quad (1.11)$$

and by setting $a = 0$, one recovers GR. This form of the theory allows one to obtain analytical expressions for the matter quantities (and therefore the energy conditions) and simplifies the general junction conditions of the theory, making it easier to perform the matching with an exterior spacetime. However, by virtue of being simple, it is also missing the potentially beneficial contributions of more complicated terms. The task of developing wormhole models with more complicated forms of $f(R, T)$ theory is left as a topic of future research.

1.2.2 Scalar-tensor representation

It is also possible to recast the geometric representation of $f(R, T)$ gravity in a dynamically equivalent scalar-tensor form, a method that has proven useful for the study of other theories of gravity [21, 25, 26]. Note that this section is based on [19] unless specified otherwise. To derive the scalar-tensor action and field equations of $f(R, T)$ theory, consider a modified action with two auxiliary fields α and β as follows:

$$S_{act} = \frac{1}{2\kappa^2} \int_{\Omega} \sqrt{-g} \left[f(\alpha, \beta) + \frac{\partial f}{\partial \alpha}(R - \alpha) + \frac{\partial f}{\partial \beta}(T - \beta) \right] d^4x + \int_{\Omega} \sqrt{-g} \mathcal{L}_m d^4x. \quad (1.12)$$

By varying this action with respect to α and β respectively, one obtains the following equations:

$$\frac{\partial^2 f}{\partial \alpha^2}(R - \alpha) + \frac{\partial^2 f}{\partial \beta \partial \alpha}(T - \beta) = 0, \quad (1.13)$$

$$\frac{\partial^2 f}{\partial \alpha \partial \beta}(R - \alpha) + \frac{\partial^2 f}{\partial \beta^2}(T - \beta) = 0. \quad (1.14)$$

²See Appendix C for details.

In matrix form, this may be written as

$$\begin{pmatrix} \frac{\partial^2 f}{\partial \alpha^2} & \frac{\partial^2 f}{\partial \beta \partial \alpha} \\ \frac{\partial^2 f}{\partial \alpha \partial \beta} & \frac{\partial^2 f}{\partial \beta^2} \end{pmatrix} \begin{pmatrix} R - \alpha \\ T - \beta \end{pmatrix} = 0. \quad (1.15)$$

The solution to this system of equations will be unique if and only if the Hessian determinant of $f(\alpha, \beta)$ does not vanish. If $f(\alpha, \beta)$ satisfies Schwartz's theorem such that $\frac{\partial^2 f}{\partial \alpha \partial \beta} = \frac{\partial^2 f}{\partial \beta \partial \alpha}$, then this condition can be written as

$$\left(\frac{\partial^2 f}{\partial \alpha^2} \right) \left(\frac{\partial^2 f}{\partial \beta^2} \right) \neq \left(\frac{\partial^2 f}{\partial \alpha \partial \beta} \right)^2. \quad (1.16)$$

In this case, the unique solution is

$$\alpha = R, \quad \beta = T. \quad (1.17)$$

Note that by substituting this solution back into the action (1.12), one recovers the $f(R, T)$ action (1.7). Now consider two scalar fields φ and ψ and an interaction potential $V(\varphi, \psi)$, which are defined as

$$\varphi = \frac{\partial f}{\partial R}, \quad \psi = \frac{\partial f}{\partial T}, \quad (1.18)$$

$$V(\varphi, \psi) = -f(\alpha, \beta) + \alpha\varphi + \beta\psi. \quad (1.19)$$

By substituting equations (1.17) and (1.19) into the action (1.12), one obtains the scalar-tensor action

$$S_{act} = \frac{1}{2\kappa^2} \int_{\Omega} \sqrt{-g} [\varphi R + \psi T - V(\varphi, \psi)] d^4x + \int_{\Omega} \sqrt{-g} \mathcal{L}_m d^4x. \quad (1.20)$$

It is apparent from equation (1.19) that a given form of the potential $V(\varphi, \psi)$ corresponds to a family of forms of the function $f(R, T)$. Indeed, by substituting equations (1.18) into equation (1.19), one obtains a partial differential equation for $f(R, T)$, which generally does not have unique solutions. Varying the action (1.20) with respect to the metric, φ and ψ respectively yields the following field equations:

$$\varphi R_{\mu\nu} - \frac{1}{2} g_{\mu\nu} [\varphi R + \psi T - V(\varphi, \psi)] + (g_{\mu\nu} \square - \nabla_{\mu} \nabla_{\nu}) \varphi = 8\pi T_{\mu\nu} - \psi (T_{\mu\nu} + \Theta_{\mu\nu}), \quad (1.21)$$

with two additional equations of motion for the scalar fields, given by

$$\frac{\partial V}{\partial \varphi} = R, \quad \frac{\partial V}{\partial \psi} = T. \quad (1.22)$$

Unlike the geometric representation, where one must choose a form of the function $f(R, T)$, one must now choose a form of the potential $V(\varphi, \psi)$ instead. Note also that the geometric field equations (1.8) are fourth-order with respect to the metric as they contain, through the derivatives of the function $f(R, T)$, the second derivative of R , which itself contains the second derivatives of the metric. In comparison, the scalar-tensor field equations (1.21) are only second-order, as they do not contain any derivatives of R . However, this comes at the cost of introducing two new equations of motion for φ and ψ , given by equations (1.22).

In this thesis, the lower order of the scalar-tensor field equations may provide a way to consider more complicated forms of $f(R, T)$ while not sacrificing the potential of obtaining analytical solutions to the matter quantities. For this reason, the scalar-tensor representation is used in this thesis for a different particular case of $f(R, T)$ theory from the one considered in the sections regarding the geometric representation, which was given by equation (1.10). For this new case, the following interaction potential is chosen:

$$V(\varphi, \psi) = m_1 \varphi^2 + m_2 \psi^2. \quad (1.23)$$

This potential is inspired by particle physics³, where the scalar fields φ and ψ would be carried by particles with masses m_1 and m_2 respectively. Note that the scalar fields do not need to represent real particles in the context of this thesis. As such, their "masses" need not be positive but can have any real nonzero values. In the case of a potential given by equation (1.23), the scalar field equations of motion (1.22) are uncoupled and simple to solve, as follows:

$$\begin{aligned} \frac{\partial V}{\partial \varphi} = 2m_1 \varphi = R &\implies \varphi = \frac{R}{2m_1}, \\ \frac{\partial V}{\partial \psi} = 2m_2 \psi = T &\implies \psi = \frac{T}{2m_2}. \end{aligned} \quad (1.24)$$

To show that the potential (1.23) represents a more complicated form of the function $f(R, T)$ than that used in the geometric case of this thesis, consider the definition (1.19). With equations

³More specifically, the Klein-Gordon Lagrangian of a system with two massive spin-0 fields; see [27], p. 355 for an example with one field.

(1.17), (1.18) and (1.23), it can be rewritten as

$$f(R, T) = R\varphi + T\psi - V(\varphi, \psi) = R\frac{\partial f}{\partial R} + T\frac{\partial f}{\partial T} - m_1 \left(\frac{\partial f}{\partial R}\right)^2 - m_2 \left(\frac{\partial f}{\partial T}\right)^2. \quad (1.25)$$

This is a particular case of the Clairaut equation for two variables [28]. To solve it, one may take the partial derivatives with respect to R and T , which results in the following system of equations:

$$\begin{aligned} \left(R - 2m_1 \frac{\partial f}{\partial R}\right) \frac{\partial^2 f}{\partial R^2} + \left(T - 2m_2 \frac{\partial f}{\partial T}\right) \frac{\partial^2 f}{\partial T \partial R} &= 0, \\ \left(T - 2m_2 \frac{\partial f}{\partial T}\right) \frac{\partial^2 f}{\partial R \partial T} + \left(R - 2m_1 \frac{\partial f}{\partial R}\right) \frac{\partial^2 f}{\partial T^2} &= 0. \end{aligned} \quad (1.26)$$

These can be rewritten in matrix form as

$$\begin{pmatrix} \frac{\partial^2 f}{\partial R^2} & \frac{\partial^2 f}{\partial T \partial R} \\ \frac{\partial^2 f}{\partial R \partial T} & \frac{\partial^2 f}{\partial T^2} \end{pmatrix} \begin{pmatrix} R - 2m_1 \frac{\partial f}{\partial R} \\ T - 2m_2 \frac{\partial f}{\partial T} \end{pmatrix} = 0. \quad (1.27)$$

As discussed above, the solution to this system of equations is unique if and only if the Hessian determinant of $f(R, T)$ does not vanish. In that case, the solution is given by

$$\begin{aligned} R - 2m_1 \frac{\partial f}{\partial R} &= 0 \implies \frac{\partial f}{\partial R} = \frac{R}{2m_1}, \\ T - 2m_2 \frac{\partial f}{\partial T} &= 0 \implies \frac{\partial f}{\partial T} = \frac{T}{2m_2}. \end{aligned} \quad (1.28)$$

These equations can be integrated with respect to R and T , which yields

$$f(R, T) = \frac{R^2}{4m_1} + F_1(T) = \frac{T^2}{4m_2} + F_2(R). \quad (1.29)$$

From this, it is clear that the integration functions $F_1(T)$ and $F_2(R)$ must be given by

$$F_1(T) = \frac{T^2}{4m_2} + \lambda_1, \quad F_2(R) = \frac{R^2}{4m_1} + \lambda_2, \quad (1.30)$$

where λ_1 and λ_2 are constants of integration. These can be associated with the cosmological constant Λ , so let $\lambda_1 = \lambda_2 = -2\Lambda$. After substituting this and the above functions into equation (1.29), one obtains

$$f(R, T) = \frac{R^2}{4m_1} + \frac{T^2}{4m_2} - 2\Lambda. \quad (1.31)$$

Unlike the form of $f(R, T)$ given by (1.10), this is quadratic in both R and T and, as such, will have significantly different physical properties, which will become evident in Chapter 2.

1.3 Thin-shell formalism and junction conditions

As stated in the introduction, the wormhole models considered in this thesis employ the thin-shell formalism, which is a method of obtaining new spacetime solutions that join (or "match") two existing spacetimes defined in complementary regions. In this thesis, the matching takes place on a 3-dimensional hypersurface Σ with a constant radius r_Σ , separating the interior (that is, inside Σ) wormhole spacetime from an exterior (outside Σ) Kottler spacetime⁴. In addition, the "+" and "-" superscripts denote whether the value of a quantity is given in the exterior or interior spacetime, respectively. If no superscript is given, the quantity may be considered a distribution function valid in the *entire* spacetime. Unless stated otherwise, this section is based on [19]. The thin-shell formalism also requires some new geometric quantities to be defined:

1. $e_a^\mu \equiv \frac{\partial x^\mu}{\partial y^a}$ are the projectors from a 4-dimensional spacetime (the interior or exterior), with the coordinates $x^\mu = (t, r, \theta, \phi)$, onto Σ , with the coordinates $y^a = (\tau, \theta, \phi)$. The corresponding inverse projectors are $e_\mu^a \equiv \frac{\partial y^a}{\partial x^\mu}$.
2. n^μ is the spacelike unit normal vector on Σ pointing from the interior to the exterior, which satisfies the normalization condition $g_{\mu\nu}n^\mu n^\nu = 1$. Note that by definition, its projection onto Σ must be zero, and as Σ is a hypersurface of constant radius, then the nonradial components of n^μ must also be zero. These properties can, respectively, be expressed as

$$e_\mu^a n^\mu = e_a^\mu n_\mu = 0, \quad n^t = n^\theta = n^\phi = 0. \quad (1.32)$$

With these, it is possible to derive the following alternative expression for n_r :

$$g_{\mu\nu}n^\mu n^\nu = g_{rr}(n^r)^2 = g^{rr}(n_r)^2 = (g_{rr})^{-1}(n_r)^2 = 1 \implies n_r = \sqrt{g_{rr}}. \quad (1.33)$$

3. $h_{ab} = e_a^\mu e_b^\nu g_{\mu\nu}$ is the **induced metric** of Σ , induced on the interior and exterior of Σ by the corresponding spacetime.

⁴This is a unified term for both de Sitter- and anti-de Sitter-Schwarzschild spacetimes.

4. $K_{ab} \equiv \nabla_a n_b = e_a^\mu e_b^\nu \nabla_\mu n_\nu$ is the **extrinsic curvature** of Σ , with $K \equiv h^{ab} K_{ab}$ being the corresponding trace.
5. S_{ab} is the stress-energy tensor of a thin-shell at Σ .
6. The **jump** of a quantity X , denoted by $[X]$, is defined as the change of X across Σ , from the interior to the exterior. Mathematically, this is defined as

$$[X] \equiv X^+|_\Sigma - X^-|_\Sigma. \quad (1.34)$$

This implies by definition that

$$[e_a^\mu] = 0 \implies e_a^{+\mu} = e_a^{-\mu} \text{ and } [n^\mu] = 0 \implies n^{+\mu} = n^{-\mu}. \quad (1.35)$$

Note that most of the above parameters have Latin indices. These are used throughout this thesis to distinguish the 3-dimensional parameters of the hypersurface from the 4-dimensional ones of the interior/exterior spacetimes, which have Greek indices.

One may now determine the requirements for matching the interior and exterior spacetimes – the junction conditions. For any given theory of gravity, these conditions may be obtained using the distribution formalism, where one first writes the metric of the *entire* spacetime as

$$g_{\mu\nu} = g_{\mu\nu}^+ H(l) + g_{\mu\nu}^- H(-l), \quad (1.36)$$

where $H(l)$ is the Heaviside step function and l is the proper distance along geodesics perpendicular to Σ , with $l < 0$ inside Σ , $l > 0$ outside Σ and $l = 0$ on Σ . One would now like to calculate the Christoffel symbols, Ricci tensor and Ricci scalar from the above metric, but doing so gives rise to terms proportional to the Dirac delta function $\delta(l) = \frac{dH(l)}{dl}$. For example, the derivatives of the metric are given by

$$\partial_\lambda g_{\mu\nu} = \partial_\lambda g_{\mu\nu}^+ H(l) + \partial_\lambda g_{\mu\nu}^- H(-l) + [g_{\mu\nu}] n_\lambda \delta(l). \quad (1.37)$$

As the Christoffel symbols feature products of the (inverse) metric and its derivatives, then evidently they will contain terms proportional to $H(l)\delta(l)$. In addition, the Riemann tensor features products of the Christoffel symbols, which will lead to terms proportional to $\delta^2(l)$.

These are either undefined or singular in the distribution formalism and, as such, must be forced to vanish using the junction conditions, which are therefore the constraints that guarantee that all quantities are well-defined in the distribution formalism.

After using the junction conditions to eliminate the undefined and singular terms in the field equations, some terms proportional to $\delta(l)$ will remain in the geometric part of the equations. Thus one should expect some similar terms in the matter part. To ensure this, one may write the stress-energy tensor of the entire spacetime as

$$T_{\mu\nu} = T_{\mu\nu}^+ H(l) + T_{\mu\nu}^- H(-l) + S_{\mu\nu} \delta(l).^5 \quad (1.38)$$

The matching may be characterised in two different ways: if the condition $S_{\mu\nu} = 0$ is also imposed, then the matching is *smooth*. If $S_{\mu\nu} \neq 0$, then there is a shell of matter at Σ , known as the *thin-shell*, that separates the interior and exterior spacetimes. Note that, in general, the explicit form of $S_{\mu\nu}$ depends on the geometric quantities defined previously.

1.3.1 Geometric representation

The first junction condition of the geometric representation of $f(R, T)$ gravity given by equation (1.10) can be derived from the fact that with derivatives of the metric of the form (1.37), the Christoffel symbols will have terms proportional to $H(l)\delta(l)$, which must be eliminated as explained above. To do this, one must impose $[g_{\mu\nu}] = 0$ as the first junction condition. Using the definition of h_{ab} and the property $[e_a^\mu] = 0$, one may also write the following:

$$[g_{\mu\nu}] e_a^\mu e_b^\nu = [g_{\mu\nu} e_a^\mu e_b^\nu] = [h_{ab}], \quad (1.39)$$

which allows the first junction condition to be restated in a more convenient way as

$$[h_{ab}] = 0. \quad (1.40)$$

To derive the second junction condition, consider that calculating $R_{\mu\nu}$ and R in the distribution formalism is done in the way given by equations (5) and (6), but using the metric given by

⁵This is not the most general form of $T_{\mu\nu}$, as it does not include the so-called double-layer terms. However, these terms vanish in the cases considered in this thesis (see [19]), and thus there is no need to include them.

equation (1.36). The results, after considering that $[g_{\mu\nu}] = 0$, are (see also [23], pp. 88-89)

$$R_{\mu\nu} = R_{\mu\nu}^+ H(l) + R_{\mu\nu}^- H(-l) - (e_\mu^a e_\nu^b [K_{ab}] + n_\mu n_\nu [K]) \delta(l), \quad (1.41)$$

$$R = R^+ H(l) + R^- H(-l) - 2[K] \delta(l). \quad (1.42)$$

One can also obtain the distributional form of T by contracting equation (1.38) with the metric:

$$T = g^{\mu\nu} T_{\mu\nu} = T^+ H(l) + T^- H(-l) + S \delta(l), \quad (1.43)$$

where $S = g^{\mu\nu} S_{\mu\nu} = h^{ab} S_{ab}$. By replacing equations (1.38), (1.41), (1.42) and (1.43) into the field equations (1.11), projecting the result onto Σ using $e_a^\mu e_b^\nu$, and cancelling out any terms not proportional to $\delta(l)$, one obtains

$$-e_a^\mu e_b^\nu (e_\mu^c e_\nu^d [K_{cd}] + n_\mu n_\nu [K]) - \frac{1}{2} e_a^\mu e_b^\nu (-2[K] + aS) g_{\mu\nu} = e_a^\mu e_b^\nu (8\pi + a) S_{\mu\nu}, \quad (1.44)$$

which can be simplified and rearranged into the second junction condition:

$$(8\pi + a) S_{ab} + \frac{a}{2} S h_{ab} = [K] h_{ab} - [K_{ab}]. \quad (1.45)$$

With this and equation (1.40), the field equations will not contain any terms proportional to $H(l)\delta(l)$ or $\delta^2(l)$, which means that no more junction conditions are required for this case.

1.3.2 Scalar-tensor representation

To derive the junction conditions of the scalar-tensor representation of $f(R, T)$ for a matching with a thin-shell and a potential of the form given by equation (1.23), consider equations (1.36), (1.37), (1.38), (1.41), (1.42) and (1.43). By the same considerations as in the geometric part, the first junction condition can be stated as

$$[h_{ab}] = 0. \quad (1.46)$$

To continue, one must define the distributional forms of the scalar fields φ and ψ , which are

$$\varphi = \varphi^+ H(l) + \varphi^- H(-l), \quad \psi = \psi^+ H(l) + \psi^- H(-l). \quad (1.47)$$

Note that these have no terms proportional to $\delta(l)$. This guarantees that the potential $V(\varphi, \psi)$ and its partial derivatives will not have any terms containing $H(l)\delta(l)$ or $\delta^2(l)$. In addition, the partial derivatives of $V(\varphi, \psi)$ depend on R and T through equations (1.22). This implies that R and T must also have no terms containing $\delta(l)$, which upon comparison with equations (1.42) and (1.43) leads to the junction conditions

$$[K] = 0, \quad S = 0. \quad (1.48)$$

The field equations (1.21) depend on the second covariant derivatives of φ , so these must also be calculated. The first covariant derivative of φ is

$$\nabla_\mu \varphi = \partial_\mu \varphi = \frac{\partial \varphi}{\partial R} \partial_\mu R. \quad (1.49)$$

With the condition $[K] = 0$, the partial derivative of R may be written in the distribution formalism as

$$\partial_\mu R = \partial_\mu R^+ H(l) + \partial_\mu R^- H(-l) + [R] n_\mu \delta(l). \quad (1.50)$$

As shown in Section 1.2, a potential given by equation (1.22) corresponds to a form of $f(R, T)$ given by equation (1.31), which is quadratic in R . This implies that to avoid terms proportional to $\delta^2(l)$ and $H(l)\delta(l)$, one must impose $[R] = 0$ in equation (1.50). Consider now the first derivative of φ in the distribution formalism:

$$\partial_\mu \varphi = \partial_\mu \varphi^+ H(l) + \partial_\mu \varphi^- H(l) + [\varphi] n_\mu \delta(l). \quad (1.51)$$

Note that since φ is linear in R , this expression is proportional to $\partial_\mu R$ by equation (1.49). The condition $[R] = 0$ therefore implies that the term proportional to $\delta(l)$ must also vanish in equation (1.51), which leads to the junction condition

$$[\varphi] = 0. \quad (1.52)$$

The second covariant derivative of φ is

$$\nabla_\mu \nabla_\nu \varphi = \frac{\partial \varphi}{\partial R} \nabla_\mu \nabla_\nu R, \quad (1.53)$$

with the corresponding distributional form, after considering that $[\varphi] = 0$, being

$$\nabla_\mu \nabla_\nu \varphi = \nabla_\mu \nabla_\nu \varphi^+ H(l) + \nabla_\mu \nabla_\nu \varphi^- H(l) + n_\mu [\partial_\nu \varphi] \delta(l). \quad (1.54)$$

By now substituting equations (1.9), (1.38), (1.41), (1.42), (1.43), (1.48), (1.52) and (1.54) into the field equations (1.21), projecting the result onto Σ using $e_a^\mu e_b^\nu$, and cancelling out the nonsingular terms as in the geometric case, one obtains the junction condition

$$(8\pi + \psi_\Sigma) S_{ab} = h_{ab} n^\mu [\partial_\mu \varphi] - \varphi_\Sigma [K_{ab}], \quad (1.55)$$

where φ_Σ and ψ_Σ are the average values of φ and ψ at the thin-shell. With the condition $[\varphi] = 0$, these may be written as

$$\varphi_\Sigma \equiv \frac{\varphi^+|_\Sigma + \varphi^-|_\Sigma}{2} = \varphi^-|_\Sigma, \quad \psi_\Sigma \equiv \frac{\psi^+|_\Sigma + \psi^-|_\Sigma}{2}. \quad (1.56)$$

The trace of equation (1.55) is

$$(8\pi + \psi_\Sigma) S = 3n^\mu [\partial_\mu \varphi] - \varphi_\Sigma [K]. \quad (1.57)$$

The conditions given by equations (1.48) imply that this equation can be rewritten as the final junction condition:

$$3n^\mu [\partial_\mu \varphi] = 0 \implies [\partial_\mu \varphi] = 0. \quad (1.58)$$

With this, one may now discard the junction condition $S = 0$ and the first term on the right-hand side of equation (1.55). In summary, the junction conditions of the scalar-tensor representation of $f(R, T)$ for a matching with a thin-shell and a potential given by equation (1.23) are

$$\begin{aligned} [h_{ab}] &= 0, \\ [K] &= 0, \\ [\varphi] &= 0, \\ [\partial_\mu \varphi] &= 0, \\ (8\pi + \psi_\Sigma) S_{ab} &= -\varphi_\Sigma [K_{ab}]. \end{aligned} \quad (1.59)$$

2 Wormhole solutions

To obtain the explicit forms of the energy conditions, one must first find solutions for the matter quantities of the wormhole: ρ , p_r and p_t . As this requires solving the field equations (1.8) (or in the scalar-tensor representation, (1.21)), then depending on the forms of $f(R, T)$ (or the potential $V(\varphi, \psi)$), $\zeta(r)$ and $b(r)$, these solutions may not be obtainable analytically and will require numerical methods. However, as the following sections show, both cases studied in this thesis have analytical solutions for the matter quantities. Furthermore, one must apply the relevant junction conditions from Section 1.3 to determine the explicit conditions for matching the interior and exterior spacetimes. All calculations in this chapter have been performed using the software *Wolfram Mathematica* [29] and the code used is provided in Appendix A. Any analytical results will be given in terms of the general functions $\zeta(r)$ and $b(r)$, but the numerical examples will use the particular forms given by equations (1.3).

Before beginning this chapter in earnest, consider the question of what value to assign to the mass M of the wormhole. It is common practice (for example, see [15]) to normalise the radial coordinate r with respect to M so that a unitless value is assigned to r/M . This has the distinct advantage of producing results valid for any value of M and will also be employed in this thesis. In addition to r and the radii r_0 and r_Σ , one must also normalise some other parameters. Through a dimensional analysis of the equations in the previous chapter, one may conclude that the normalised parameters must be defined as follows:

$$\bar{r}_0 = \frac{r_0}{M}, \quad \bar{r}_\Sigma = \frac{r_\Sigma}{M}, \quad \bar{m}_1 = m_1 M^2, \quad \bar{m}_2 = m_2 M^2, \quad \bar{\Lambda} = \Lambda M^2. \quad (2.1)$$

Note that in the case of $\bar{\Lambda}$ the factor M^2 is not evident from the previous chapter. However, the following section will show that the metric of the Kottler spacetime contains a term proportional to Λr^2 , which must be unitless. This directly implies that Λ must be normalised with respect to M as given above.

2.1 Geometric representation

2.1.1 Matter quantities

As mentioned in Section 1.2, the field equations (1.11) are analytically solvable for the matter quantities. By solving the field equations, one obtains the following expressions:

$$\rho = \frac{C_1}{r^2} \left\{ a \left[(4r - 3b(r))\zeta'(r) + r(r - b(r)) (\zeta'(r)^2 + 2\zeta''(r)) \right] + b'(r) \left[16(a + 6\pi) - ar\zeta'(r) \right] \right\}, \quad (2.2)$$

$$p_r = \frac{C_1}{r^2} \left\{ \left[a(8 + r\zeta'(r))b'(r) + 4(5a + 24\pi)r\zeta'(r) - ar^2 (\zeta'(r)^2 + 2\zeta''(r)) \right] + \frac{b(r)}{r} \left[-24(a + 4\pi) - 3(7a + 32\pi)r\zeta'(r) + ar^2 (\zeta'(r)^2 + 2\zeta''(r)) \right] \right\}, \quad (2.3)$$

$$p_t = \frac{C_1}{r^2} \left\{ \left[- \left(4(a + 12\pi) + (5a + 24\pi)r\zeta'(r) \right) b'(r) + 8(a + 6\pi)r\zeta'(r) + (5a + 24\pi)r^2 (\zeta'(r)^2 + 2\zeta''(r)) \right] + \frac{b(r)}{r} \left[12(a + 4\pi) - 3(a + 8\pi)r\zeta'(r) - (5a + 24\pi)r^2 (\zeta'(r)^2 + 2\zeta''(r)) \right] \right\}, \quad (2.4)$$

where $C_1 \equiv [24(a + 4\pi)(a + 8\pi)]^{-1}$. These quantities will satisfy the NEC and WEC at the throat with a suitable choice of parameters, which is not possible in GR. For example:

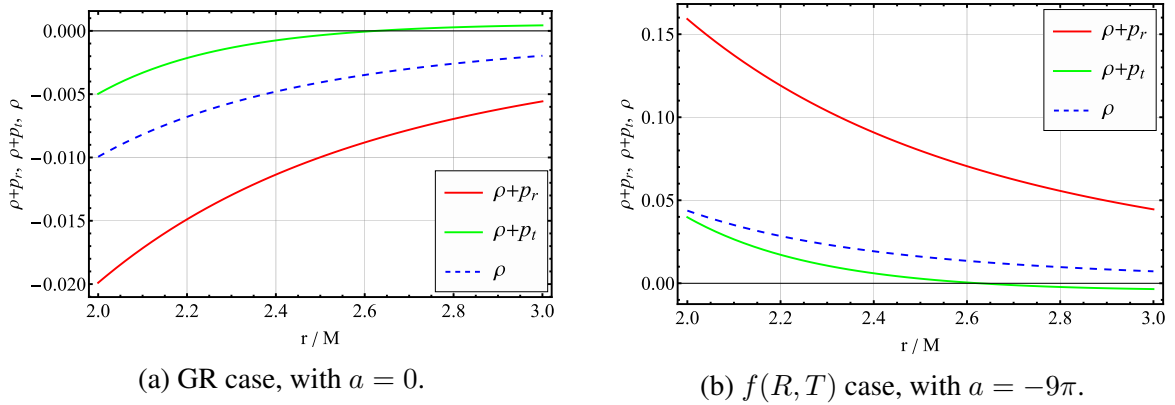


Figure 2.1: The WEC parameters as functions of the mass-normalised radius r/M , henceforth referred to as "WEC-s," with the parameters $\zeta_0 = \alpha = \beta = 1$ and $\bar{r}_0 = 2$. Two different cases for the value of a are presented, as described in the corresponding subcaptions.

Figure 2.1b shows that in the $f(R, T)$ case, the transverse part of the NEC ($\rho + p_t \geq 0$) is satisfied only close to the throat. Indeed, there exists no currently known set of parameters for this particular case with which the NEC is satisfied everywhere. As such, one must turn to the

thin-shell formalism to exclude the region where this condition is violated.

2.1.2 Spacetime matching

To determine the explicit forms of the junction conditions, one must first calculate the induced metric and extrinsic curvature of the hypersurface Σ on both the interior and exterior sides. The coordinates θ and ϕ are the same in the entire spacetime, so only the time coordinate changes from the interior to the exterior. By defining the time coordinate in the interior as $t^- = e^{-\frac{1}{2}\zeta(r_\Sigma)}\tau$, one obtains the projectors from the interior to Σ , given by

$$e^{-\mu}_a = \begin{pmatrix} e^{-\frac{1}{2}\zeta(r_\Sigma)} & 0 & 0 \\ 0 & 0 & 0 \\ 0 & 1 & 0 \\ 0 & 0 & 1 \end{pmatrix}. \quad (2.5)$$

Using this and equation (1.1) with $r = r_\Sigma$, one may obtain the interior induced metric as

$$h^-_{ab} = e^\alpha_a e^\beta_b g_{\alpha\beta} = \begin{pmatrix} -1 & 0 & 0 \\ 0 & r_\Sigma^2 & 0 \\ 0 & 0 & r_\Sigma^2 \sin^2 \theta \end{pmatrix}. \quad (2.6)$$

The same procedure must now be performed for the exterior Kottler spacetime. Consider the following Kottler metric:

$$g^+_{\mu\nu} = \begin{pmatrix} -\left(1 - \frac{2M}{r} - \frac{\Lambda}{3}r^2\right) e^{\zeta_e} & 0 & 0 & 0 \\ 0 & \left(1 - \frac{2M}{r} - \frac{\Lambda}{3}r^2\right)^{-1} & 0 & 0 \\ 0 & 0 & r^2 & 0 \\ 0 & 0 & 0 & r^2 \sin^2 \theta \end{pmatrix}, \quad (2.7)$$

where ζ_e is an arbitrary constant, M is the mass of the wormhole, and Λ is the cosmological constant. Consider also the exterior time coordinate $t^+ = \left(1 - \frac{2M}{r_\Sigma} - \frac{\Lambda}{3}r_\Sigma^2\right)^{-1/2} e^{-\frac{1}{2}\zeta_e}\tau$, which

provides the following projectors:

$$e^{+\mu}_a = \begin{pmatrix} \left(1 - \frac{2M}{r_\Sigma} - \frac{\Lambda}{3}r_\Sigma^2\right)^{-1/2} e^{-\frac{1}{2}\zeta_e} & 0 & 0 \\ 0 & 0 & 0 \\ 0 & 1 & 0 \\ 0 & 0 & 1 \end{pmatrix}. \quad (2.8)$$

As with the interior spacetime, one may now set $r = r_\Sigma$ in equation (2.7) and use the projectors (2.8) to obtain the exterior induced metric as

$$h^+_{ab} = e^\alpha_a e^\beta_b g^+_{\alpha\beta} = \begin{pmatrix} -1 & 0 & 0 \\ 0 & r_\Sigma^2 & 0 \\ 0 & 0 & r_\Sigma^2 \sin^2 \theta \end{pmatrix}. \quad (2.9)$$

When comparing the induced metrics (2.6) and (2.9), it is evident that the junction condition $[h_{ab}] = 0$ is satisfied. As $[e^\mu_a] = 0$ by definition, then the projectors (2.5) and (2.8) must be equal. This leads to the following condition:

$$\begin{aligned} e^{\zeta(r_\Sigma)} &= e^{\zeta_e} \left(1 - \frac{2M}{r_\Sigma} - \frac{\Lambda}{3}r_\Sigma^2\right) \Rightarrow \\ \Rightarrow \zeta_e &= \ln \left(\frac{e^{\zeta(r_\Sigma)}}{1 - \frac{2M}{r_\Sigma} - \frac{\Lambda}{3}r_\Sigma^2} \right) = \zeta(r_\Sigma) - \ln \left(1 - \frac{2M}{r_\Sigma} - \frac{\Lambda}{3}r_\Sigma^2\right), \end{aligned} \quad (2.10)$$

Note that as ζ_e is arbitrary, it may always be chosen such that this condition is satisfied for a given r_Σ . In other words, this condition places no constraints on choosing a value for r_Σ .

The second junction condition contains the extrinsic curvature K_{ab} , which depends on n_μ . Using equation (1.33) with the metrics (1.1) and (2.7), one can write the radial components of n_μ as

$$n_r^+ = \frac{1}{\sqrt{1 - \frac{b(r)}{r}}}, \quad n_r^- = \frac{1}{\sqrt{1 - \frac{2M}{r} - \frac{\Lambda}{3}r^2}}. \quad (2.11)$$

The extrinsic curvatures can now be calculated. After calculating the covariant derivative, one must set $r = r_\Sigma$ to obtain results valid on Σ , which yields the following:

$$K_{ab}^- = e_a^{-\mu} e_b^{-\nu} \nabla_\mu n_\nu^- = \sqrt{1 - \frac{b(r_\Sigma)}{r_\Sigma}} \begin{pmatrix} -\frac{\zeta'(r_\Sigma)}{2} & 0 & 0 \\ 0 & r_\Sigma & 0 \\ 0 & 0 & r_\Sigma \sin^2 \theta \end{pmatrix}, \quad (2.12)$$

$$K_{ab}^+ = e_a^{+\mu} e_b^{+\nu} \hat{\nabla}_\mu n_\nu^+ = \sqrt{1 - \frac{2M}{r_\Sigma} - \frac{\Lambda}{3} r_\Sigma^2} \begin{pmatrix} -\frac{3M - \Lambda r_\Sigma^3}{3r_\Sigma^2 \left(1 - \frac{2M}{r_\Sigma} - \frac{\Lambda}{3} r_\Sigma^2\right)} & 0 & 0 \\ 0 & r_\Sigma & 0 \\ 0 & 0 & r_\Sigma \sin^2 \theta \end{pmatrix}. \quad (2.13)$$

Note that K_{ab}^+ is defined in the exterior spacetime, which means that the covariant derivative must be defined in terms of the metric (2.7). This is indicated here by $\hat{\nabla}_\mu$. The corresponding traces are

$$K^- = h^{ab} K_{ab}^- = \frac{4 + r_\Sigma \zeta'(r_\Sigma)}{2r_\Sigma} \sqrt{1 - \frac{b(r_\Sigma)}{r_\Sigma}}, \quad (2.14)$$

$$K^+ = h^{ab} K_{ab}^+ = \frac{2r_\Sigma - 3M - \Lambda r_\Sigma^3}{r_\Sigma^2 \sqrt{1 - \frac{2M}{r_\Sigma} - \frac{\Lambda}{3} r_\Sigma^2}}. \quad (2.15)$$

The second junction condition (1.45) can now be solved for the stress-energy tensor S_{ab} of the thin-shell. To calculate the energy conditions, one must first calculate $S^a_b = h^{ac} S_{bc}$, the nontrivial components of which correspond to the energy density and surface pressures of the thin-shell, denoted by σ and p respectively, as

$$\sigma = -S^\tau_\tau = S_{\tau\tau} = -\frac{C_2}{r_\Sigma^2} \left\{ \frac{(a + 16\pi)r_\Sigma - (a + 32\pi)M - \frac{2}{3}(a + 8\pi)\Lambda r_\Sigma^3}{\sqrt{1 - \frac{2M}{r_\Sigma} - \frac{\Lambda}{3} r_\Sigma^2}} - r_\Sigma [2a + 32\pi + a r_\Sigma \zeta'(r_\Sigma)] \sqrt{1 - \frac{b(r_\Sigma)}{r_\Sigma}} \right\}, \quad (2.16)$$

$$p = S^\theta_\theta = \frac{1}{r_\Sigma^2} S_{\theta\theta} = \frac{C_2}{r_\Sigma^2} \left\{ \frac{(3a + 16\pi)r_\Sigma - (5a + 16\pi)M - \frac{4}{3}(a + 8\pi)\Lambda r_\Sigma^3}{\sqrt{1 - \frac{2M}{r_\Sigma} - \frac{\Lambda}{3} r_\Sigma^2}} - r_\Sigma \left[3a + 16\pi - \left(\frac{a}{2} + 8\pi\right) r_\Sigma \zeta'(r_\Sigma) \right] \sqrt{1 - \frac{b(r_\Sigma)}{r_\Sigma}} \right\}, \quad (2.17)$$

$$S^\phi_\phi = \frac{1}{r_\Sigma^2 \sin^2 \theta} S_{\phi\phi} = S^\theta_\theta = p, \quad (2.18)$$

where $C_2 \equiv [(a - 16\pi)(a + 8\pi)]^{-1}$. Note that the WEC of the thin-shell is

$$\sigma \geq 0, \quad \sigma + p \geq 0, \quad (2.19)$$

where the second inequality is the NEC of the thin-shell.

One must also choose values for \bar{r}_Σ and $\bar{\Lambda}$ to perform the matching. Consider a particular example with the parameters $\zeta_0 = \alpha = \beta = 1$, $\bar{r}_0 = 3$ and $a = -9\pi$. By now solving the WEC inequalities of the wormhole spacetime and the thin-shell with respect to \bar{r}_Σ and $\bar{\Lambda}$, one finds that they are all satisfied if the following conditions are met:

$$3 < \bar{r}_\Sigma \leq 3.9393, \quad \frac{3(28\bar{r}_\Sigma^3 - 3\bar{r}_\Sigma^2 - 63\bar{r}_\Sigma - 54)}{\bar{r}_\Sigma^3(\bar{r}_\Sigma + 3)(2\bar{r}_\Sigma + 3)^2} \leq \bar{\Lambda} < \frac{3(\bar{r}_\Sigma - 2)}{\bar{r}_\Sigma^3}. \quad (2.20)$$

One may now choose a suitable value of \bar{r}_Σ and then calculate the interval of explicit values for $\bar{\Lambda}$. For example, choosing $\bar{r}_\Sigma = 3.5$ yields $0.095726 \leq \bar{\Lambda} < 0.10496$, so one may choose $\bar{\Lambda} = 0.1$ for the matching. The WEC plots for this case are presented in Figure 2.2.

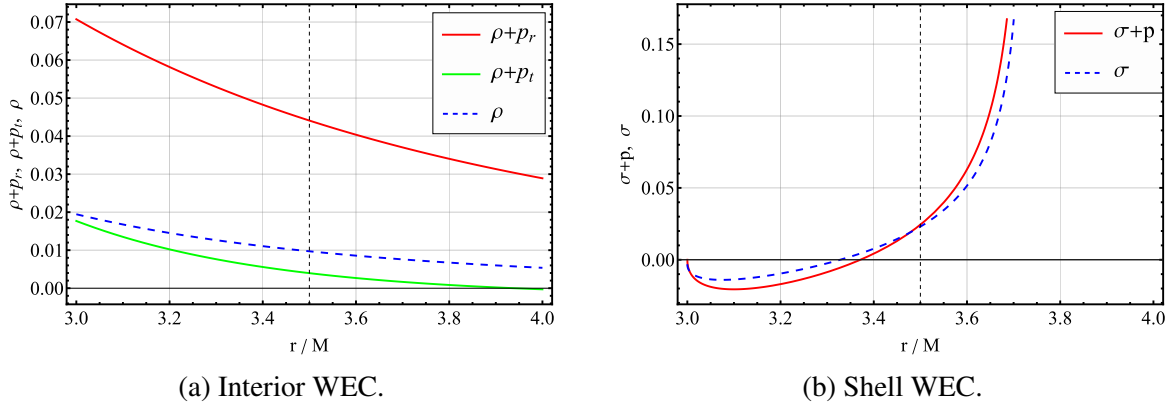


Figure 2.2: The WEC-s of an interior wormhole spacetime (left) and thin-shell (right), with the parameters $\zeta_0 = \alpha = \beta = 1$, $\bar{r}_0 = 3$, $a = -9\pi$, $\bar{\Lambda} = 0.1$. The matching radius $\bar{r}_\Sigma = 3.5$ is denoted with a vertical dashed line.

From these figures, one may see that a matching with these parameters produces a spacetime where the NEC and WEC are satisfied everywhere. Note that substituting the parameters chosen in this example into equation (2.10) gives $\zeta_e \approx 4.7573$.

2.2 Scalar-tensor representation

2.2.1 Matter quantities

Similarly to the geometric representation, the scalar-tensor field equations (1.21) can be solved immediately for the matter quantities, implying that the solutions will be functions of φ (and its first and second derivatives), ψ and $V(\varphi, \psi)$. Therefore, after choosing a specific form of $V(\varphi, \psi)$, one must use equations (1.22) to determine the explicit forms of φ and ψ , which in turn can be used to find the explicit forms of the matter quantities. In this thesis, φ and ψ are given by equations (1.24). Using equations (1.4) and (1.5), one may rewrite them as

$$\varphi = \frac{R}{2m_1} = \frac{[r\zeta'(r) + 4]b'(r) + [3b(r) - 4r]\zeta'(r) + r[b(r) - r][\zeta'(r)^2 + 2\zeta''(r)]}{4m_1r^2}, \quad (2.21)$$

$$\psi = \frac{T}{2m_2} = \frac{p_r + 2p_t - \rho}{2m_2}. \quad (2.22)$$

From this, it is clear that φ is a function of only the radial coordinate r . Equation (2.22) can be fully solved by calculating the first and second derivatives of φ , substituting them alongside equation (2.21) into the solutions for the matter quantities obtained from the field equations, then substituting the results into equation (2.22) and solving for ψ . The resulting equation gives the explicit form of ψ as a function of only r , which will not be written here due to its size. Finally, by substituting the explicit forms of equation (2.21), its first and second derivatives, and equation (2.22) into the solutions for the matter quantities, one may obtain their explicit forms, which are also not shown due to their size. Note that this derivation assumes a particular form for $V(\varphi, \psi)$, but not $\zeta(r)$ or $b(r)$. A numerical example is presented in Figure 2.3.

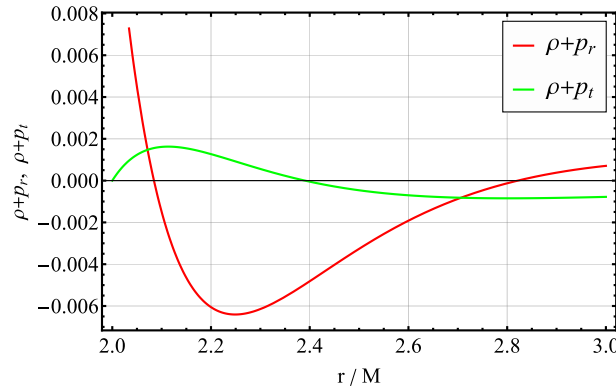


Figure 2.3: The NEC of a scalar-tensor representation wormhole spacetime, with the parameters $\bar{r}_0 = \alpha = 2$ and $\zeta_0 = \beta = \bar{m}_1 = \bar{m}_2 = 1$.

As in the geometric case, the NEC is only satisfied close to the throat, thereby motivating the use of the thin-shell formalism.

2.2.2 Spacetime matching

To solve the junction conditions given by equations (1.59), consider the same projectors and metrics as in the previous section. Following the same procedure, explicit forms can be found for the first two junction conditions. The condition $[h_{ab}] = 0$ is again satisfied by equation (2.10), and the condition $[K] = 0$ with equations (2.14) and (2.15) becomes

$$4 - \frac{6M}{r_\Sigma} - 2\Lambda r_\Sigma^2 - [4 + r_\Sigma \zeta'(r_\Sigma)] \sqrt{1 - \frac{b(r_\Sigma)}{r_\Sigma}} \sqrt{1 - \frac{2M}{r_\Sigma} - \frac{\Lambda}{3} r_\Sigma^2} = 0. \quad (2.23)$$

To solve this equation, one must also determine the explicit form of the cosmological constant Λ . For this, consider the scalar-tensor representation of the Kottler spacetime, which has arbitrary constant scalar fields φ^+ and ψ^+ [15] and, in this case, a potential of the form given by equation (1.23). This means that the field equations (1.21) in the absence of matter become

$$\begin{aligned} \varphi^+ R_{\mu\nu} - \frac{1}{2} g_{\mu\nu} \left(\varphi^+ R - m_1 \varphi^{+2} - m_2 \psi^{+2} \right) = \\ = \varphi^+ \left(R_{\mu\nu} - \frac{1}{2} R g_{\mu\nu} \right) - \frac{m_1 \varphi^{+2} + m_2 \psi^{+2}}{2} g_{\mu\nu} = 0. \end{aligned} \quad (2.24)$$

After dividing both sides of this equation by φ^+ , one arrives at Einstein's vacuum field equations, with a cosmological constant given by

$$\Lambda = -\frac{m_1 \varphi^{+2} + m_2 \psi^{+2}}{2\varphi^+} = -\frac{1}{2} \left(m_1 \varphi^+ + m_2 \frac{\psi^{+2}}{\varphi^+} \right). \quad (2.25)$$

As stated above, φ^+ and ψ^+ are arbitrary constants. This means that the junction condition $[\varphi] = 0$ can be satisfied by imposing the following equality:

$$\varphi^+ = \varphi^-|_\Sigma = \varphi_\Sigma = \text{const.} \quad (2.26)$$

This also implies that $\partial_\mu \varphi^+ = 0$, so the fourth junction condition in (1.59) becomes

$$[\partial_\mu \varphi] = \partial_\mu \varphi|_{r=r_\Sigma} = \frac{\partial \varphi}{\partial r} \Big|_{r=r_\Sigma} = 0. \quad (2.27)$$

The explicit form of this equation is

$$\begin{aligned}
& b''(r_\Sigma) [4r_\Sigma + r_\Sigma^2 \zeta'(r_\Sigma)] + b'(r_\Sigma) \{-8 + r_\Sigma \zeta'(r_\Sigma) [2 + r_\Sigma \zeta'(r_\Sigma)] + 3r_\Sigma^2 \zeta'''(r_\Sigma)\} + \\
& + b(r_\Sigma) \{r_\Sigma [-\zeta'(r_\Sigma)^2 + \zeta''(r_\Sigma) + 2r_\Sigma \zeta'''(r_\Sigma)] - 2\zeta'(r_\Sigma) [3 - r_\Sigma^2 \zeta''(r_\Sigma)]\} + \\
& + 2r_\Sigma \{\zeta'(r_\Sigma) [2 - r_\Sigma^2 \zeta''(r_\Sigma)] - r_\Sigma [2\zeta''(r_\Sigma) + r_\Sigma \zeta'''(r_\Sigma)]\} = 0.
\end{aligned} \tag{2.28}$$

Note that at this point, ψ^+ remains arbitrary. This means that one may choose an arbitrary value for Λ and assign a value to ψ^+ that satisfies equation (2.25). By solving this equation for ψ^+ and substituting equation (2.26) into it, one obtains the following expression:

$$\psi^+ = \sqrt{-\frac{m_1 \varphi_\Sigma^2 + 2\varphi_\Sigma \Lambda}{m_2}}. \tag{2.29}$$

This result implies that there exist two possible values of ψ^+ for any given value of Λ , one positive and one negative. In addition, ψ^+ will have imaginary values for some combinations of parameters. In this thesis, any cases with imaginary values are discarded, and the positive value of ψ^+ is used in further calculations. Finally, one must numerically solve equations (2.23) and (2.28) for \bar{r}_Σ and ζ_0 to perform a matching.¹ For this, one must choose values for \bar{r}_0 , α , β , $\bar{\Lambda}$, \bar{m}_1 and \bar{m}_2 and consider that $\bar{r}_\Sigma > \bar{r}_0$. In this thesis, an algorithm was used that attempted the matching for all possible combinations of the following parameter values:

$$\begin{aligned}
\bar{r}_0 &= \frac{j}{2}, \quad j = 4, 5, 6 \dots, 10, \\
\alpha &= \frac{k}{2}, \quad k = 0, 1, 2 \dots, 20, \\
\beta &= \frac{l}{2}, \quad l = -1, 0, 1 \dots, 20, \\
\bar{\Lambda} &\in \{-1, 0, 1\}, \\
\bar{m}_1 &= \pm 1, \\
\bar{m}_2 &= \pm 1.
\end{aligned} \tag{2.30}$$

As solving equations (2.23) and (2.28) may take a very long time in some cases (for example, with large half-integer values of α or β), an upper time limit of 5 minutes was imposed for any particular solution calculation time to prevent the algorithm from freezing.

¹Theoretically one could solve them for \bar{r}_Σ and any parameter other than \bar{m}_1 or \bar{m}_2 as long as the rest are given, but ζ_0 was chosen due to the junction conditions being at most quadratic in it and therefore simple to solve.

For each combination of parameters, the algorithm either failed to solve equations (2.23) and (2.28) or succeeded and produced one or more pairs of values for ζ_0 and \bar{r}_Σ . In addition, the algorithm checked whether a given calculated ζ_0 and \bar{r}_Σ with the associated initial parameters produced a real value of ψ^+ and resulted in solutions for the matter quantities that satisfied the NEC of the wormhole spacetime in the interval $\bar{r}_0 \leq \bar{r} \leq \bar{r}_\Sigma$.² If these conditions were met, then the NEC of the thin-shell was also checked. For this, the last junction condition in (1.59) was converted to the following form:

$$S^a_b = h^{ac} S_{bc} = -\frac{\varphi_\Sigma}{8\pi + \psi_\Sigma} h^{ac} [K_{bc}], \quad (2.31)$$

and solved explicitly for S^a_b using the parameter values. Like in the geometric case, the energy density and surface pressure of the thin-shell correspond to the components of S^a_b as

$$\sigma = -S^\tau_\tau, \quad p = S^\theta_\theta = S^\phi_\phi. \quad (2.32)$$

Finally, if the NEC of the interior spacetime was satisfied, then its WEC was checked alongside the shell's WEC. Two particular examples of matching attempts are presented in Figure 2.4.

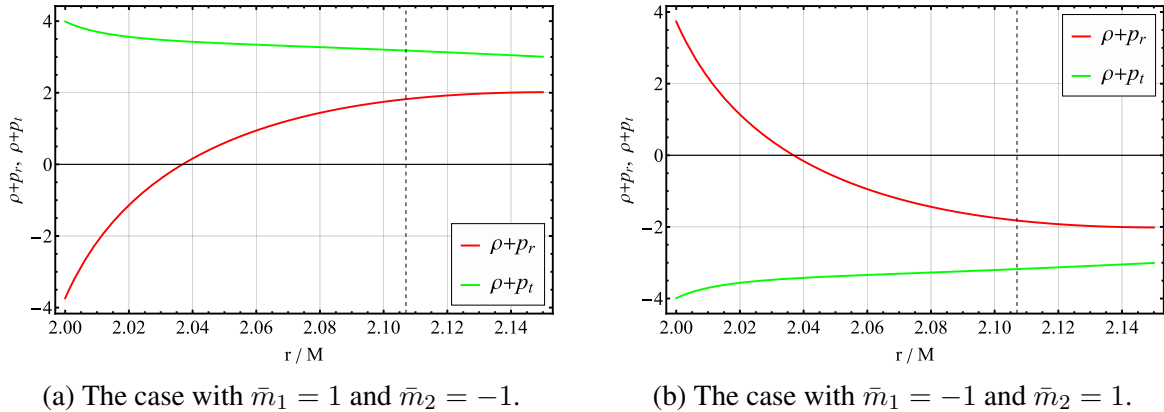


Figure 2.4: The NEC-s of the interior wormhole spacetimes of two scalar-tensor representation matching attempts, with the initial parameters $\bar{r}_0 = \alpha = 2$, $\beta = 1$, $\bar{\Lambda} = 0$ and $\zeta_0 \approx -6.7990$. The parameters \bar{m}_1 and \bar{m}_2 are given in the corresponding subcaptions. In both cases, the vertical dashed line denotes the matching radius $\bar{r}_\Sigma \approx 2.1070$.

The complete set of results is presented in Appendix B. In summary, no combination of parameters produced a result that satisfied the NEC of the wormhole spacetime within the matching radius. Therefore, the WEC is automatically violated in every case, and checking the validity of the shell energy conditions is also unnecessary.

²This was actually done at 5 evenly spaced points, including \bar{r}_0 and \bar{r}_Σ , to save computational time.

Conclusions

This thesis aimed to develop new traversable wormhole models in the geometric and scalar-tensor representations of $f(R, T)$ gravity that satisfy the NEC everywhere, using the thin-shell formalism. This was successful in the geometric case, with the model also satisfying the WEC everywhere. The thin-shell formalism was crucial for this, emphasising its usefulness in developing such models. The particular form of $f(R, T)$ theory used in this case was also a commonly used form due to its simplicity (see [12] for an example), which increases the applicability of the results of this thesis in other fields of research.

The scalar-tensor case used in this thesis used a more complicated form of $f(R, T)$ theory. In this case, no model was found that satisfied the NEC everywhere. This was attempted with a large set of different initial parameters, which provides a strong case for concluding that this may not be possible for the combination of the scalar field interaction potential $V(\varphi, \psi)$ and redshift and shape functions $\zeta(r)$ and $b(r)$ used in this thesis. It is possible that different forms of these functions, or some untested set of initial parameters, may result in a model that indeed satisfies the NEC everywhere. The task of confirming this is left as a topic of future research.

The thin-shell formalism was used in this thesis to develop wormhole models that satisfy the NEC everywhere. However, one would also like to do so without the thin-shell formalism, as was done in [17], for example. Indeed, the form of $f(R, T)$ used in this article was the same as in the geometric case of this thesis, which implies that similar results may be possible. It is unlikely that the same applies to the scalar-tensor case, as discussed in the previous paragraph. Instead, one may have to turn to different forms of $V(\varphi, \psi)$, $\zeta(r)$ and $b(r)$. In such cases, the respective field equations and junction conditions may not be analytically solvable and will instead require numerical methods. Finally, one could also employ the Palatini formalism. The junction conditions of Palatini $f(\mathcal{R}, T)$ gravity (see [30]) are less restrictive than those of the metric formalism used in this thesis and, as such, may permit new and interesting solutions.

Acknowledgements

First and foremost, I would like to thank my supervisor João Luís Rosa for his support and constant help with any problems and questions I had, be it about writing this thesis or simply satisfying my curiosity regarding some nuance of theoretical physics. His feedback was always quick yet incredibly constructive. Second, I would also like to thank assistant prof. Laur Järv for his help with translating some of the terms used here into Estonian. Finally, my deepest thanks go to my family and friends both in and outside the University of Tartu for all the jokes and discussions I have had with them over the years and for always being ready to lend an ear when asked. Without them, I would not be where or who I am today.

Paul Martin Kull

Bibliography

- [1] R. d’Inverno. *Introducing Einstein’s Relativity*. Clarendon Press, 1992. ISBN: 978-0-19-859686-8.
- [2] S. M. Carroll et al. “Is cosmic speed-up due to new gravitational physics?” In: *Physical Review D* 70.4 (Aug. 2004). Publisher: American Physical Society (APS). DOI: 10 . 1103/physrevd.70.043528.
- [3] E. Elizalde et al. “Nonsingular exponential gravity: A simple theory for early- and late-time accelerated expansion”. In: *Phys. Rev. D* 83.8 (Apr. 2011). Publisher: American Physical Society. DOI: 10 . 1103/PhysRevD.83.086006.
- [4] S. Capozziello, V. F. Cardone and A. Troisi. “Dark energy and dark matter as curvature effects?” In: *Journal of Cosmology and Astroparticle Physics* 2006.08 (Aug. 2006). Publisher: IOP Publishing, pp. 001–001. DOI: 10 . 1088/1475–7516/2006/08/001.
- [5] C. F. Martins and P. Salucci. “Analysis of rotation curves in the framework of R_n gravity”. In: *Monthly Notices of the Royal Astronomical Society* 381.3 (Oct. 2007). Publisher: Oxford University Press (OUP), pp. 1103–1108. DOI: 10 . 1111/j . 1365–2966 . 2007.12273.x.
- [6] C. G. Boehmer, T. Harko and F. S. N. Lobo. “Dark matter as a geometric effect in $f(R)$ gravity”. In: *Astroparticle Physics* 29.6 (July 2008). Publisher: Elsevier BV, pp. 386–392. DOI: 10.1016/j.astropartphys.2008.04.003.
- [7] S. Capozziello, A. Stabile and A. Troisi. “Newtonian limit of $f(R)$ gravity”. In: *Physical Review D* 76.10 (Nov. 2007). Publisher: American Physical Society (APS). DOI: 10 . 1103/physrevd.76.104019.

- [8] G. J. Olmo. “Limit to general relativity in $f(R)$ theories of gravity”. In: *Physical Review D* 75.2 (Jan. 2007). Publisher: American Physical Society (APS). DOI: 10.1103/physrevd.75.023511.
- [9] S. Nojiri and S. D. Odintsov. “Unified cosmic history in modified gravity: From theory to Lorentz non-invariant models”. In: *Physics Reports* 505.2-4 (Aug. 2011). Publisher: Elsevier BV, pp. 59–144. DOI: 10.1016/j.physrep.2011.04.001.
- [10] T. Harko et al. “ $f(R,T)$ gravity”. In: *Physical Review D* 84.2 (July 2011). Publisher: American Physical Society (APS). DOI: 10.1103/physrevd.84.024020.
- [11] R. Zaregonbadi, M. Farhoudi and N. Riazi. “Dark matter from $f(R,T)$ gravity”. In: *Physical Review D* 94.8 (Oct. 2016). Publisher: American Physical Society (APS). DOI: 10.1103/physrevd.94.084052.
- [12] S. Dey, A. Chanda and B. C. Paul. “Compact objects in $f(R, T)$ gravity with Finch–Skea geometry”. In: *The European Physical Journal Plus* 136.2 (Feb. 2021), p. 228. ISSN: 2190-5444. DOI: 10.1140/epjp/s13360-021-01173-w.
- [13] H. Velten and T. R. P. Caramês. “Cosmological inviability of $f(R,T)$ gravity”. In: *Physical Review D* 95.12 (June 2017). Publisher: American Physical Society (APS). DOI: 10.1103/physrevd.95.123536.
- [14] B. Mishra et al. “Traversable wormhole models in $f(R)$ gravity”. In: *International Journal of Modern Physics A* 37.05 (Feb. 2022). Publisher: World Scientific Pub Co Pte Ltd. DOI: 10.1142/s0217751x22500105.
- [15] J. L. Rosa, J. P. S. Lemos and F. S. N. Lobo. “Wormholes in generalized hybrid metric-Palatini gravity obeying the matter null energy condition everywhere”. In: *Physical Review D* 98.6 (Sept. 2018). arXiv: 1808.08975. ISSN: 2470-0010, 2470-0029. DOI: 10.1103/PhysRevD.98.064054.
- [16] H. Maeda. “Simple traversable wormholes violating energy conditions only near the Planck scale”. In: *Classical and Quantum Gravity* 39.7 (Mar. 2022). Publisher: IOP Publishing. DOI: 10.1088/1361-6382/ac586b.
- [17] A. Banerjee, M.K. Jasim and S. G. Ghosh. “Wormholes in $f(R,T)$ gravity satisfying the null energy condition with isotropic pressure.” In: *Annals of Physics* 433 (2021). ISSN: 0003-4916. DOI: 10.1016/j.aop.2021.168575.

- [18] A. Dixit, C. Chawla and A. Pradhan. “Traversable wormholes with logarithmic shape function in $f(R,T)$ gravity”. In: *International Journal of Geometric Methods in Modern Physics* 18.04 (Feb. 2021). Publisher: World Scientific Pub Co Pte Lt. DOI: 10.1142/s021988782150064x.
- [19] J. L. Rosa. “Junction conditions and thin-shells in perfect-fluid $f(R,T)$ gravity”. In: *Physical Review D* 103.10 (May 2021). arXiv: 2103.11698. ISSN: 2470-0010, 2470-0029. DOI: 10.1103/PhysRevD.103.104069.
- [20] M. R. Mehdizadeh, M. K. Zangeneh and F. S. N. Lobo. “Einstein-Gauss-Bonnet traversable wormholes satisfying the weak energy condition”. In: *Physical Review D* 91.8 (Apr. 2015). Publisher: American Physical Society (APS). DOI: 10.1103/physrevd.91.084004.
- [21] A. Bakopoulos, C. Charmousis and P. Kanti. “Traversable wormholes in beyond Horndeski theories”. In: *Journal of Cosmology and Astroparticle Physics* 2022.05 (May 2022). Publisher: IOP Publishing, p. 022. DOI: 10.1088/1475-7516/2022/05/022.
- [22] J. Sadeghi et al. “Traversable wormhole in logarithmic $f(R)$ gravity by various shape and redshift functions”. In: *International Journal of Modern Physics D* 31.03 (Jan. 2022). Publisher: World Scientific Pub Co Pte Ltd. DOI: 10.1142/s0218271822500195.
- [23] E. Poisson. *A Relativist’s Toolkit: The Mathematics of Black-Hole Mechanics*. Cambridge: Cambridge University Press, 2004. ISBN: 978-0-521-83091-1. DOI: 10.1017/CBO9780511606601.
- [24] M. Visser. *Lorentzian Wormholes: From Einstein to Hawking*. Computational and Mathematical Physics. New York: Springer-Verlag, 1996. ISBN: 978-1-56396-394-0.
- [25] T. B. Gonçalves, J. L. Rosa and F. S. N. Lobo. “Cosmology in scalar-tensor $f(R,T)$ gravity”. In: *Physical Review D* 105.6 (Mar. 2022). Publisher: American Physical Society (APS). DOI: 10.1103/physrevd.105.064019.
- [26] T. B. Gonçalves, J. L. Rosa and F. S. N. Lobo. “Cosmological sudden singularities in $f(R,T)$ gravity”. In: *The European Physical Journal C* 82.5 (May 2022). Publisher: Springer Science and Business Media LLC. DOI: 10.1140/epjc/s10052-022-10371-4.
- [27] D. Griffiths. *Introduction to Elementary Particles*. Second, Revised Edition. Wiley, 2008. ISBN: 978-3-527-61847-7.

- [28] *Clairaut equation*. URL: https://encyclopediaofmath.org/index.php?title=Clairaut_equation (visited on 02/05/2022).
- [29] *Wolfram Mathematica*. URL: <https://www.wolfram.com/mathematica/> (visited on 02/05/2022).
- [30] J. L. Rosa and D. Rubiera-Garcia. “Junction conditions of Palatini $f(R,T)$ gravity”. 2022. DOI: 10.48550/arXiv.2204.12944.

A *Wolfram Mathematica* code

Some extra notes for the following code:

1. The code must be run in descending order.
2. The code itself is commented in greater detail (see sentences inside "(**)").
3. The calculations in this code are performed using a unit mass $M = 1$. This creates results that are simpler to analyse within the code itself while being numerically equivalent to the more general mass-normalised results presented in this thesis.

Definitions

```
In[1]:= (*Definition of the wormhole metric*)
g := DiagonalMatrix[{-Exp[red[r]], (1 - b[r] / r) ^ -1, r^2, r^2 * Sin[th]^2}]

In[2]:= (*Definitions of the functions of the theory*)
f[Rvar_, Tvar_] := Rvar + a1 * Tvar
V[scphivar_, scpsivar_] := m1 * scphivar^2 + m2 * scpsivar^2
red[r_] := e0 * (r0 / r) ^ e
b[r_] := r0 * (r0 / r) ^ B

In[6]:= (*Definitions of basic geometric quantities in terms of the wormhole metric*)
gI = Inverse[g];
gD = D[g, {{t, r, th, phi}}];
Ct = Table[1 / 2 Sum[gI[[k]][i] * (gD[[l]][i][m] + gD[[m]][i][l] - gD[[l]][m][i]), {i, 4}],
  {k, 4}, {l, 4}, {m, 4}];
DCt = D[Ct, {{t, r, th, phi}}];
RieT = Table[-DCt[[k]][l][m][n] + DCt[[k]][l][n][m] +
  Sum[-Ct[[i]][l][m] * Ct[[k]][i][n] + Ct[[i]][l][n] * Ct[[k]][i][m], {i, 4}],
  {k, 4}, {l, 4}, {m, 4}, {n, 4}];
RicT = TensorContract[RieT, {{1, 3}}];
R = Simplify[Sum[Sum[gI[[k]][l] * RicT[[k]][l], {k, 4}], {l, 4}]];

In[13]:= (*General covariant derivative function in terms of
  the wormhole metric and a rounding function for later use*)
Cov[A_, i_ : {"0"}] := D[A, {{t, r, th, phi}}] + Sum[
  If[i[[k]] == "d", -Transpose[Ct, 1 ↔ 3].A, If[i[[k]] == "u", Transpose[Ct, 2 ↔ 3].A, 0]],
  {k, ArrayDepth[A, AllowedHeads → List]}]
GeneralRound[x_, i_ : 7] := If[x ≠ "", Round[10^i * x] * 10^(-i), ""];

In[15]:= (*Definitions of the wormhole stress-energy and θ tensors*)
Tud = DiagonalMatrix[{-rho[r], pr[r], pt[r], pt[r]}];
T = Simplify[TensorContract[Tud, {1, 2}]];
Tdd = g.Tud;
Theta = Simplify[-2 Tdd + (2 pt[r] + pr[r]) / 3 * g];
```

Geometric solutions

```
In[26]:= (*Geometric field equations and the matter quantity solutions derived from them*)
FEq = Table[Simplify[
  (D[f[Rvar, Tvar], Rvar] /. {Rvar → R, Tvar → T}) * RicT[[i]][i] - 1 / 2 f[R, T] * g[[i]][i] -
  Cov[Cov[(D[f[Rvar, Tvar], Rvar] /. {Rvar → R, Tvar → T}), {"d"}][i][i] +
  g[[i]][i] * Sum[gI[[j]][j] *
    Cov[Cov[(D[f[Rvar, Tvar], Rvar] /. {Rvar → R, Tvar → T}), {"d"}][j][j],
    {j, 4}] = 8 π * Tdd[[i]][i] - (D[f[Rvar, Tvar], Tvar] /. {Rvar → R, Tvar → T}) *
    (Tdd[[i]][i] + Theta[[i]][i])], {i, 4}];
SimpleGSOL = Solve[FEq, {rho[r], pr[r], pt[r]}];
```

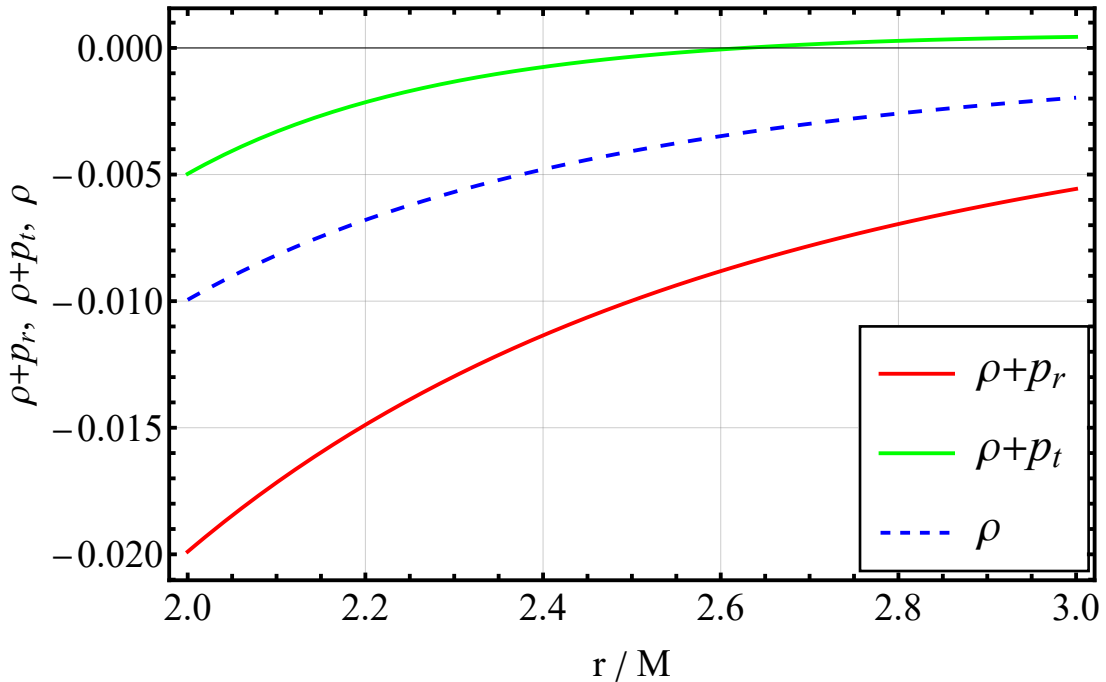


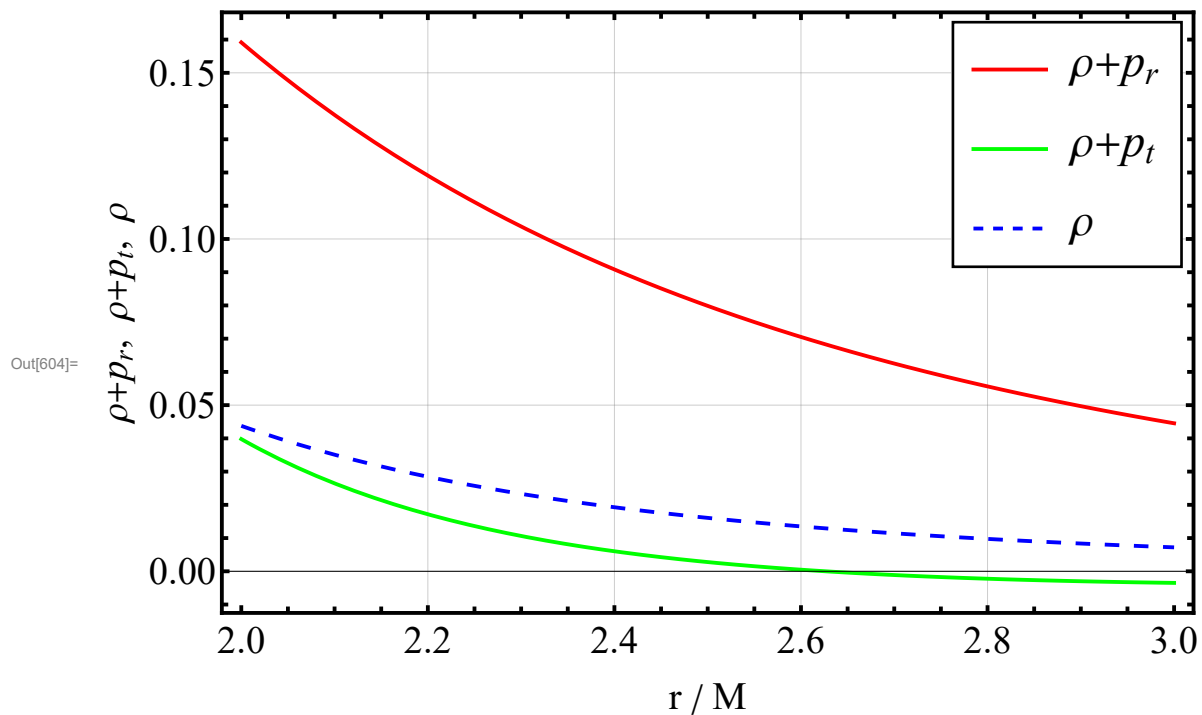
```

In[599]:= (*Example plots, including the GR case*)
Gpar = {r0 → 2, e0 → 1, e → 1, B → 1, M → 1};
EC0G[r_] = rho[r] /. SimpleGSOL;
EC1G[r_] = rho[r] + pr[r] /. SimpleGSOL;
EC2G[r_] = rho[r] + pt[r] /. SimpleGSOL;
PlotMax = 3;
(*Adjust this variable to change the maximum
value of r/M displayed on the following plots*)
(*GR case*)
Plot[{EC1G[r] /. Gpar /. a1 → 0, EC2G[r] /. Gpar /. a1 → 0, EC0G[r] /. Gpar /. a1 → 0},
{r, 2, PlotMax}, GridLines → Automatic, Ticks → Automatic,
PlotLegends → Placed[LineLegend[{"ρ+pr", "ρ+pt", "ρ"},
LegendFunction → (Framed[#, Background → White] &), LegendMargins → 5],
{0.87, 0.23}], Framelabel → {"r / M", "ρ+pr", "ρ+pt", "ρ"},
BaseStyle → {FontFamily → "Times New Roman", 20},
LabelStyle → {FontFamily → "Times New Roman"},
Frame → True, FrameStyle → Directive[Black, Thick],
PlotStyle → {{Thick, Red}, {Thick, Green}, {Blue, Dashing[0.015], Thick}},
ImageSize → Large, Epilog → Infiniteline[{1, 0}, {1, 0}]]
(*f(R,T) case*)
Plot[{EC1G[r] /. Gpar /. a1 → -9 π, EC2G[r] /. Gpar /. a1 → -9 π,
EC0G[r] /. Gpar /. a1 → -9 π}, {r, 2, PlotMax}, GridLines → Automatic,
Ticks → Automatic, PlotLegends → Placed[LineLegend[{"ρ+pr", "ρ+pt", "ρ"},
LegendFunction → (Framed[#, Background → White] &), LegendMargins → 5],
{0.87, 0.78}], Framelabel → {"r / M", "ρ+pr", "ρ+pt", "ρ"},
BaseStyle → {FontFamily → "Times New Roman", 20},
LabelStyle → {FontFamily → "Times New Roman"},
Frame → True, FrameStyle → Directive[Black, Thick],
PlotStyle → {{Thick, Red}, {Thick, Green}, {Blue, Dashing[0.015], Thick}},
ImageSize → Large, Epilog → Infiniteline[{1, 0}, {1, 0}]]

```

Out[603]=





Scalar - Tensor solutions

```

In[119]:= (*Scalar-tensor field equations and solutions for the matter quantities*)
FEqST = Table[Simplify[scphi[r] * RicT[[i]][[i]] -
  1/2 g[[i]][[i]] * (scphi[r] * R + scpsi[r] * T - V[scphi[r], scpsi[r]]) -
  Cov[Cov[scphi[r], ], {"d"}][[i]][[i]] +
  g[[i]][[i]] * Sum[gI[[j]][[j]] * Cov[Cov[scphi[r], ], {"d"}][[j]][[j]], {j, 4}] ==
  8 π * Tdd[[i]][[i]] - scpsi[r] * (Tdd[[i]][[i]] + Theta[[i]][[i]]), {i, 4}];
FEqSST = Solve[{FEqST[[1]], FEqST[[2]], FEqST[[3]]}, {rho[r], pr[r], pt[r]]][[1]] // Simplify;

In[121]:= (*Equations and solutions for the scalar fields
and explicit solutions for the matter quantities*)
EQphi = D[V[scphi[r], scpsi[r]], scphi[r]] == R;
EQpsi = D[V[scphi[r], scpsi[r]], scpsi[r]] == T;
SOLphi = Solve[EQphi //. FEqSST, scphi[r]][[1, 1]] // Simplify;
SOLpsi = Solve[EQpsi //. FEqSST //. Flatten[{SOLphi, D[SOLphi, r], D[SOLphi, r, r]}] //
  Simplify, scpsi[r]][[1, 1]];
SOLall = FEqSST //. Flatten[{SOLpsi, SOLphi, D[SOLphi, r], D[SOLphi, r, r]}];

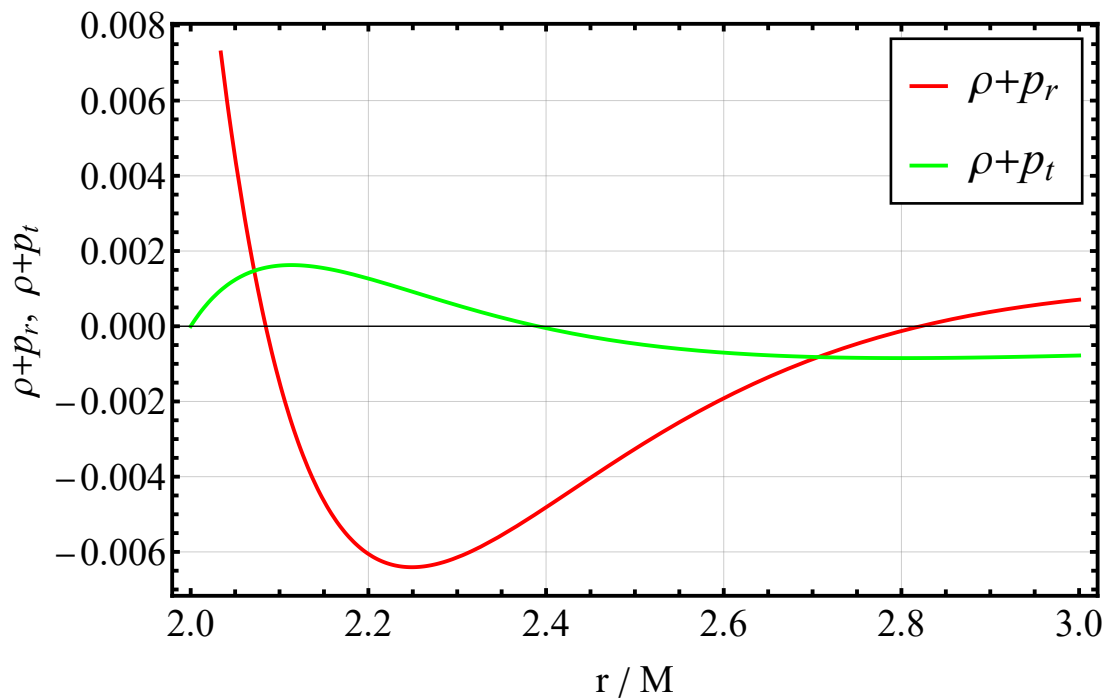
```

```

In[559]:= (*Example plot*)
STpar = {r0 → 2, e0 → 1, e → 2, B → 1, m1 → 1, m2 → 1};
EC1[r_] = rho[r] + pr[r] /. SOLall /. STpar;
EC2[r_] = rho[r] + pt[r] /. SOLall /. STpar;
PlotMax = 3;
(*Adjust this variable to change the maximum
value of r/M displayed on the following plot*)
Plot[{EC1[r] /. STpar, EC2[r] /. STpar}, {r, 2, PlotMax},
GridLines → Automatic, Ticks → Automatic, PlotLegends → Placed[
LineLegend[{" $\rho+p_r$ ", " $\rho+p_t$ "}, LegendFunction → (Framed[#, Background → White] &),
LegendMargins → 5], {0.88, 0.83}], FrameLabel → {"r / M", " $\rho+p_r$ ,  $\rho+p_t$ "},
BaseStyle → {FontFamily → "Times New Roman", 20},
LabelStyle → {FontFamily → "Times New Roman"},
Frame → True, FrameStyle → Directive[Black, Thick],
PlotStyle → {{Thick, Red}, {Green, Thick}},
ImageSize → Large, Epilog → Infiteline[1, 0], {1, 0}]

```

Out[562]=



Junction conditions

Outer Kottler

```
In[217]:= (*Geometric quantities, covariant derivative, induced metric, projectors,
normal vector and extrinsic curvature for the exterior spacetime*)
gS = DiagonalMatrix[
  {- (1 - 2 M / r - Δ / 3 * r^2), (1 - 2 M / r - Δ / 3 * r^2)^-1, r^2, r^2 * Sin[th]^2}];
gIS = Inverse[gS];
gDS = D[gS, {{t, r, th, phi}}];
CtS =
  Table[1 / 2 Sum[gIS[[k]][[i]] * (gDS[[l]][[i]][[m]] + gDS[[m]][[i]][[l]] - gDS[[l]][[m]][[i]]), {i, 4}],
    {k, 4}, {l, 4}, {m, 4}];
CovS[A_, i_ : {"θ"}] :=
  D[A, {{t, r, th, phi}}] + Sum[If[i[[k]] == "d", -Transpose[CtS, 1 ↔ 3].A, If[i[[k]] == "u",
    Transpose[CtS, 2 ↔ 3].A, 0]], {k, ArrayDepth[A, AllowedHeads → List]}}
hS = DiagonalMatrix[{-1, r^2, r^2 * Sin[th]^2}];
hIS = Inverse[hS];
evecS = D[{(1 - 2 M / r - Δ / 3 * r^2)^(-1 / 2) τ, r, th, phi}, {{τ, th, phi}}];
nS = {0, Sqrt[1 / (1 - 2 M / r - Δ / 3 * r^2)], 0, 0};
KS = Table[Sum[Simplify[CovS[nS, {"d"}]][[k, l]] × evecS[[k, i]] × evecS[[l, j]],
  {k, 4}, {l, 4}], {i, 3}, {j, 3}];
KtrS = Tr[hIS.KS] // Simplify;
```

Inner wormhole

```
In[228]:= (*Induced metric, projectors,
normal vector and extrinsic curvature for the interior spacetime*)
h = DiagonalMatrix[{-1, r^2, r^2 * Sin[th]^2}];
hI = Inverse[h];
evec = D[{Exp[red[r]]^(-1 / 2) τ, r, th, phi}, {{τ, th, phi}}];
n = {0, Sqrt[1 / (1 - b[r] / r)], 0, 0};
K = Table[Sum[Simplify[Cov[n, {"d"}]][[k, l]] × evec[[k, i]] × evec[[l, j]], {k, 4}, {l, 4}],
  {i, 3}, {j, 3}];
Ktr = Simplify[Tr[hI.K]] // Simplify;
```

Junction conditions

Geometric junction conditions

```
In[234]:= (*First geometric junction condition*)
GJC1 = SolveValues[Exp[red[r]] == Exp[ee] (1 - 2 M / r - Δ / 3 * r^2), ee][[1, 1]] /. C[1] → 0;
(*Second junction condition and thin-shell stress-energy tensor*)
SGdd = DiagonalMatrix[{SG1[r], SG2[r], SG3[r]}];
SGSOL = Solve[SGdd (8 π + a1) - 1 / 2 h * a1 * TensorContract[hI.SGdd, {1, 2}] ==
  h (KtrS - Ktr) - (KS - K), {SG1[r], SG2[r], SG3[r]}][[1]] // Simplify;
SG = hI.SGdd /. SGSOL;
```

```

In[550]:= (*Example used in the main body of the work, set a1 to 0 to see GR case*)
Gpar2 = {r0 → 3, e0 → 1, e → 1, B → 1, a1 → -9 π, M → 1};
(*Calculation to find the intervals for the values for Δ and rz in
which both the WECs of the wormhole and thin-shell are satisfied*)
GAEq = Reduce[
  ({rho[r] + pt[r] ≥ 0, -SG[[1, 1]] ≥ 0, -SG[[1, 1]] + SG[[2, 2]] ≥ 0, r > 2} /. SimpleGSOL /.
    Gpar2 // Simplify) [[1]], Δ] // Simplify // N
GAEq[[2]] /. r → 3.5
(*The interval of values for Δ in which both the WECs of the wormhole and thin-
shell are satisfied, for a matching radius of rz=3.5*)
GJC1 /. Gpar2 /. {r → 3.5, Δ → 0.1} (*Value of ge when Δ=0.1*)
Gshell0[r_] = -SG[[1, 1]] /. Gpar2 /. Δ → 0.1 // Simplify;
Gshell1[r_] = -SG[[1, 1]] + SG[[2, 2]] /. Gpar2 /. Δ → 0.1 // Simplify;
PlotMax = 4; (*Adjust this variable to change the
maximum value of r/M displayed on the following plots*)
(*On these plots the thin vertical dashed
line indicates the matching radius used in the work*)
Plot[{EC1G[r] /. Gpar2, EC2G[r] /. Gpar2, EC0G[r] /. Gpar2},
  {r, 3, PlotMax}, GridLines → Automatic, Ticks → Automatic,
  PlotLegends → Placed[LineLegend[{"ρ+pr", "ρ+pt", "ρ"},
    LegendFunction → (Framed[#, Background → White] &), LegendMargins → 5],
    {0.87, 0.77}], FrameLabel → {"r / M", "ρ+pr", "ρ+pt", "ρ"},
  BaseStyle → {FontFamily → "Times New Roman", 20},
  LabelStyle → {FontFamily → "Times New Roman"},
  Frame → True, FrameStyle → Directive[Black, Thick],
  PlotStyle → {{Thick, Red}, {Thick, Green}, {Blue, Dashing[0.015], Thick}},
  ImageSize → Large,
  Epilog → {{Dashed, InfiniteLine[{3.5, 0}, {0, 1}]}, InfiniteLine[{1, 0}, {1, 0}]}]
Plot[{Gshell1[r], Gshell0[r]}, {r, 3, PlotMax},
  GridLines → Automatic, Ticks → Automatic, PlotLegends →
    Placed[LineLegend[{"σ+p", "σ"}, LegendFunction → (Framed[#, Background → White] &),
      LegendMargins → 5], {0.89, 0.84}], FrameLabel → {"r / M", "σ+p", "σ"},
  BaseStyle → {FontFamily → "Times New Roman", 20},
  LabelStyle → {FontFamily → "Times New Roman"},
  Frame → True, FrameStyle → Directive[Black, Thick],
  PlotStyle → {{Thick, Red}, {Blue, Dashing[0.015], Thick}}, ImageSize → Large,
  Epilog → {{Dashed, InfiniteLine[{3.5, 0}, {0, 1}]}, InfiniteLine[{1, 0}, {1, 0}]}]

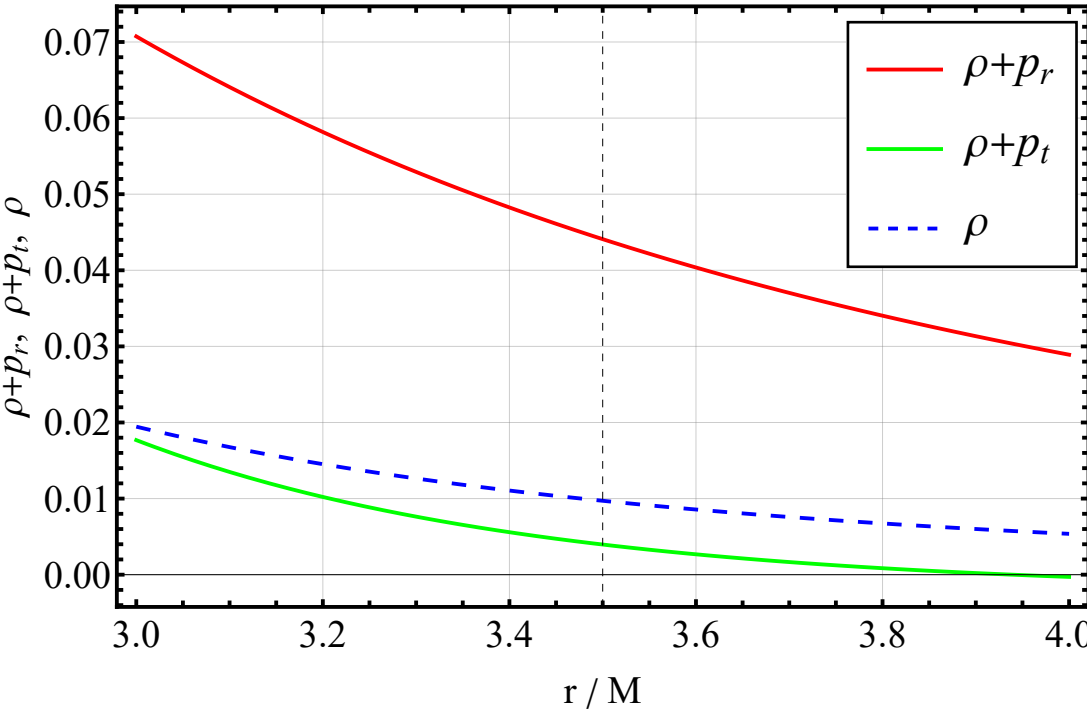
Out[551]= 3. < r ≤ 3.9393 &&  $\frac{3. (-54. - 63. r - 3. r^2 + 28. r^3)}{r^3 (3. + r) (3. + 2. r)^2} \leq \Delta < \frac{3. (-2. + r)}{r^3}$ 

Out[552]= 0.0957255 ≤ Δ < 0.104956

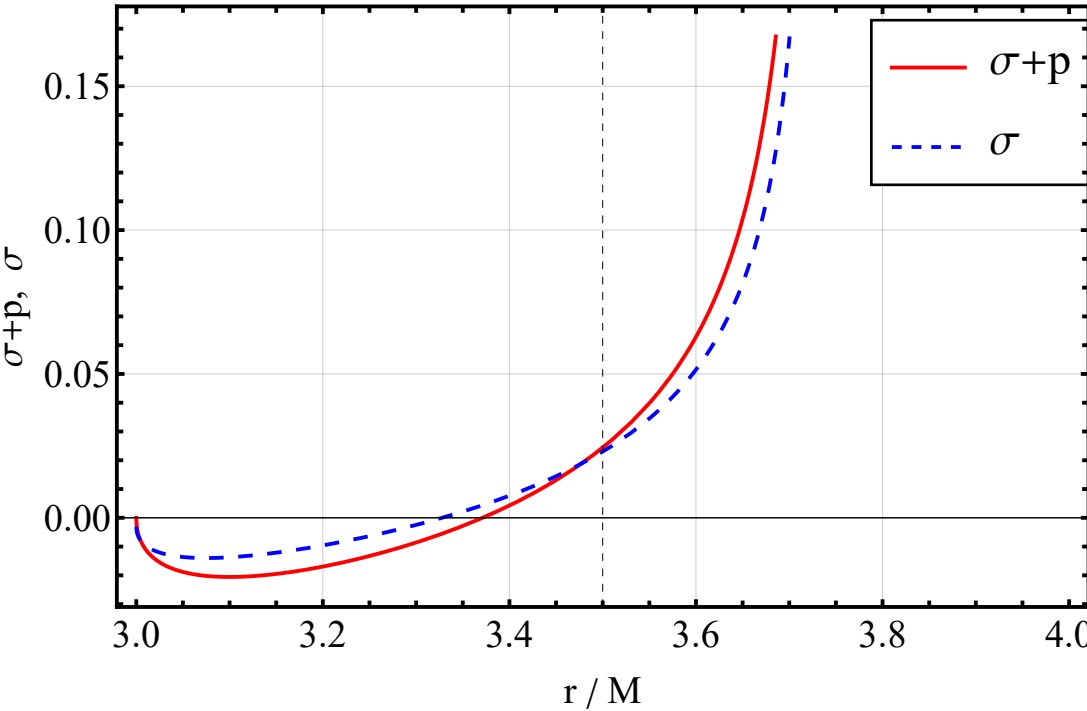
Out[553]= 4.75733

```

Out[557]=



Out[558]=

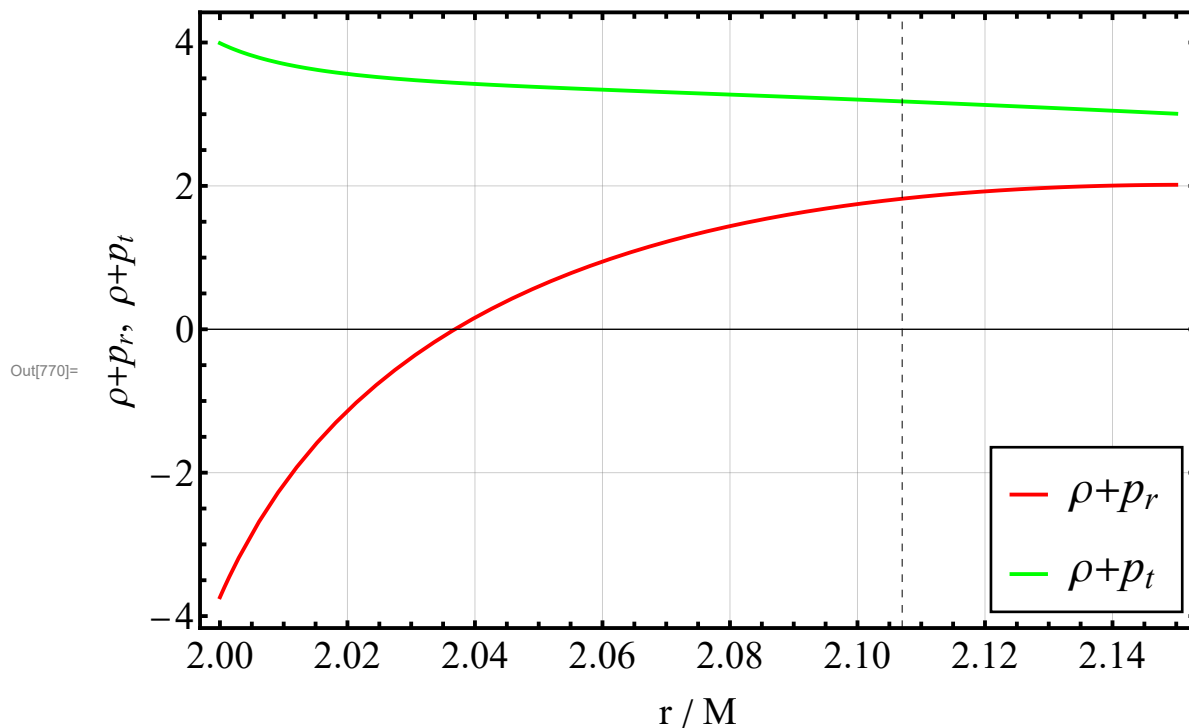


Scalar - tensor matching algorithm

```

In[758]:= (*Example matching attempt*)
JCpar = {r0 → 2, e → 2, B → 1, m1 → 1, m2 → -1, M → 1, Λ → 0};
JCEQ1 = Together[D[SOLphi, r][[2]][[4]] == 0 /. r → rΣ;
JCEQ2 = Together[KtrS - Ktr][[4]] == 0 /. r → rΣ;
SolTimer =
  AbsoluteTiming[NSolveValues[{JCEQ1, JCEQ2, rΣ > 2} /. JCpar, {rΣ, e0}, Reals]];
JCsolVal = DeleteDuplicatesBy[SolTimer[[2]], GeneralRound];
SolNumber = Length[JCsolVal];
JCsol = Table[{rΣ → JCsolVal[[i, 1]], e0 → JCsolVal[[i, 2]], {i, SolNumber}}];
JCparList = Table[Flatten[{JCpar, JCsol[[i]]}], {i, SolNumber}];
JCpar2 = JCparList[[1]];
EC1JC[r_] = rho[r] + pr[r] /. SOLall /. JCpar2;
EC2JC[r_] = rho[r] + pt[r] /. SOLall /. JCpar2;
PlotMax = 2.15;
(*On this plot the vertical dashed line indicates
the matching radius of this particular attempt*)
Plot[{EC1JC[r] // Chop, EC2JC[r] // Chop}, {r, 2, PlotMax},
GridLines → Automatic, Ticks → Automatic, PlotLegends → Placed[
  LineLegend[{"ρ+pr", "ρ+pt"}, LegendFunction → (Framed[#, Background → White] &),
  LegendMargins → 5], {0.89, 0.16}], FrameLabel → {"r / M", "ρ+pr, ρ+pt"},
BaseStyle → {FontFamily → "Times New Roman", 20},
LabelStyle → {FontFamily → "Times New Roman"},
Frame → True, FrameStyle → Directive[Black, Thick],
PlotStyle → {{Thick, Red}, {Green, Thick}}, ImageSize → Large, Epilog →
  {{Dashed, InfiniteLine[{rΣ /. JCpar2, 0}, {0, 1}], InfiniteLine[{1, 0}, {1, 0}]}]
(*Scalar field values at the thin-shell for φ,
ψ and ψ+ respectively. Chop commands are required to remove floating-
point calculation errors that introduce complex values*)
SOLphi[[2]] /. r → rΣ /. JCpar2 // Chop
SOLpsi[[2]] /. r → rΣ /. JCpar2 // Chop
psiΣ = 1 / 2 *  $\left( \text{SOLpsi}[[2]] + \sqrt{-\frac{m1 * \text{SOLphi}[[2]]^2 + 2 * \text{SOLphi}[[2]] * \Lambda}{m2}} \right) /. r \rightarrow r\Sigma /. JCpar2 // Chop$ 
(*Thin-shell stress-energy tensor*)
S = ((-SOLphi[[2]]) / (8 π + psiΣ)) hI. (K - KS) /. r → rΣ /. JCpar2 // Chop // MatrixForm

```



Out[771]= -2.14644

Out[772]= -26.353

Out[773]= -12.1033

Out[774]/MatrixForm=

$$\begin{pmatrix} -0.01396 & 0 & 0 \\ 0 & 0.00697999 & 0 \\ 0 & 0 & 0.00697999 \end{pmatrix}$$

```
(*Algorithm to attempt matching with various initial
parameters. The results are collected into a file called
"Matching.csv" in the same directory as this notebook*)
writeStream = OpenWrite["Matching.csv", PageWidth -> Infinity, FormatType -> StandardForm]
AttemptCounter = 0; (*Counter to help keep track of how far the calculations are*)
Monitor[Do[Clear[StatsToPrint, StatsToPrintFail];
  r0test = r0var / 2;
  etest = evar / 2;
  Btest = Bvar / 2;
  JCpar = {r0 -> r0test, e -> etest, B -> Btest, M -> 1, Δ -> Δvar};
  (*The following two junction conditions
  are solved for  $\xi_0$  and  $r_\Sigma$  with a time limit of 5 minutes*)
  JCEQ1 = Together[D[SOLphi, r][[2]][[4]] == 0 /. r -> rΣ];
  JCEQ2 = Together[KtrS - Ktr][[4]] == 0 /. r -> rΣ;
  SolTimer = TimeConstrained[
    AbsoluteTiming[NSolveValues[{JCEQ1, JCEQ2, rΣ > r0test} /. JCpar, {rΣ, e0}, Reals]],
    300, {Write[writeStream, StringRiffle[{AttemptCounter++, r0, e, B, Δ, "",
      "", "", "", "", "", "", "", "", "False"} /. JCpar, "", "], Continue[]]}];
  If[Length[SolTimer[[2]]] == 0, {Write[writeStream,
    StringRiffle[{AttemptCounter++, r0, e, B, Δ, "", "", "", "", "", "", "", "", "False",
      "", "", "", "", "", GeneralRound[SolTimer[[1]]} /. JCpar, "", "], Continue[]]}];
```



```

JCSol = DeleteDuplicatesBy[SolTimer[[2]], GeneralRound];
(*This command helps remove most duplicate solutions*)
Do[EVTimer = AbsoluteTiming[ Catch[JCpar2 =
    Flatten[{JCpar, {m1 → m1var, m2 → m2var, rΣ → JCSol[[i, 1]], e0 → JCSol[[i, 2]]}}];
    (*Calculation of scalar fields and check to see if ψ+ is real*)
    phiΣ = SOLphi[[2]] /. r → rΣ /. JCpar2 // Chop;
    psie =  $\sqrt{-\left(m1var * phiΣ^2 + 2 phiΣ * \Lambda var\right) / m2var}$  // Chop;
    NECs = "";
    WECs = "";
    NECss = "";
    WECss = "";
    psieIs = "";
    psiΣ = "";
    ξe = "";
    Clear[StatsToPrint];
    If[Im[psie] == 0, psieIs = "True", {psieIs = "False", Throw[Null]}];
    psiΣ = 1 / 2 * (SOLpsi[[2]] + psie) /. r → rΣ /. JCpar2 // Chop;
    ξe = Log[ -  $\left( \left( 3 e^{e0} \left( \frac{r0}{rΣ} \right)^e rΣ \right) / (6 M - 3 rΣ + rΣ^3 \Lambda) \right)$  ] /. JCpar2 // Chop;

    (*Calculation of the constant ξe*)
    (*Calculation of enegy conditions*)
    EC0JC[r_] = rho[r] /. SOLall /. JCpar2;
    EC1JC[r_] = rho[r] + pr[r] /. SOLall /. JCpar2;
    EC2JC[r_] = rho[r] + pt[r] /. SOLall /. JCpar2;
    NECcount = 0;
    WECcount = 0;
    rΣtest = rΣ /. JCpar2;
    (*Check to see if the wormhole NEC is satisfied*)
    Do[{EC1Test = EC1JC[rtest] // Chop, EC2Test = EC2JC[rtest] // Chop,
        If[Im[EC1Test] ≠ 0 || EC1Test < 0, Break[], NECcount++],
        If[Im[EC2Test] ≠ 0 || EC2Test < 0, Break[], NECcount++]},
        {rtest, r0test, rΣtest, (rΣtest - r0test) / 4}];
    If[NECcount == 5, NECs = "True", {NECs = "False", Throw[Null]}];
    (*Check of shell energy conditions and wormhole WEC*)
    S = ((-phiΣ) / (8 π + psiΣ)) hI. (K - KS) /. r → rΣ /. JCpar2 // Chop;
    If[Im[S[[1, 1]]] == 0 && Im[S[[2, 2]]] == 0, If[-S[[1, 1]] + S[[2, 2]] ≥ 0,
        {NECss = "True", WECss = -S[[1, 1]] ≥ 0}, {NECss = "False", WECss = "False"}];
    Do[{EC0Test = EC0JC[rtest] // Chop, If[Im[EC0Test] ≠ 0 || EC0Test < 0, Break[],
        WECcount++]}, {rtest, r0test, rΣtest, (rΣtest - r0test) / 4}];
    WECs = WECcount == 5];

    (*Writing out the collected results of this attempt into the csv file*)
    StatsToPrint =
    MapAt[GeneralRound, {AttemptCounter++, r0, e, B, Λ, e0, rΣ, m1, m2, phiΣ, psiΣ, psie,
        ξe, "True", psieIs, NECs, WECs, NECss, WECss, SolTimer[[1]], EVTimer[[1]]} /. JCpar2,
        {{6}, {7}, {10}, {11}, {12}, {13}, {20}, {21}}];
    Write[writeStream, StringRiffle[StatsToPrint, ","],
        {i, Length[JCSol]}, {m1var, {-1, 1}}, {m2var, {-1, 1}}, {r0var, 4, 10},
        {evar, 0, 20}, {Bvar, -1, 20}, {Λvar, -1, 1}], {AttemptCounter, JCpar}]
Close[writeStream]

```

B Scalar-tensor matching data

The complete set of matching data is too large to be included here directly, so it has been uploaded in the form of an Excel spreadsheet and can be accessed from the following link:

<https://www.dropbox.com/s/gpp7q967m7h0xda>

C Derivation for the explicit form of $\Theta_{\mu\nu}$

As noted in Section 1.2, the tensor $\Theta_{\mu\nu}$ is defined as $\Theta_{\mu\nu} \equiv g^{\alpha\beta} \frac{\delta T_{\alpha\beta}}{\delta g^{\mu\nu}}$. If one assumes that the stress-energy tensor does not depend on the first- or higher-order derivatives of the metric, then it may be written as

$$T_{\mu\nu} = -\frac{2}{\sqrt{-g}} \frac{\delta(\sqrt{-g}\mathcal{L}_m)}{\delta g^{\mu\nu}} = g_{\mu\nu}\mathcal{L}_m - 2\frac{\partial\mathcal{L}_m}{\partial g^{\mu\nu}}. \quad (\text{C.1})$$

After substituting this into the definition for $\Theta_{\mu\nu}$ and performing the variational calculations (see [10] for details), one obtains the following:

$$\Theta_{\mu\nu} = g_{\mu\nu}\mathcal{L}_m - 2T_{\mu\nu} - 2g^{\alpha\beta} \frac{\partial^2\mathcal{L}_m}{\partial g^{\mu\nu} \partial g^{\alpha\beta}}. \quad (\text{C.2})$$

In the case of an anisotropic perfect fluid and the sign convention chosen in this thesis, the matter Lagrangian may be defined as $\mathcal{L}_m = \frac{1}{3}(p_r + 2p_t)$. Substituting this into the previous equation yields

$$\Theta_{\mu\nu} = -2T_{\mu\nu} + \frac{1}{3}(p_r + 2p_t)g_{\mu\nu}, \quad (\text{C.3})$$

which is the same as equation (1.9).

Non-exclusive licence to reproduce the thesis and make the thesis public

I, Paul Martin Kull

1. grant the University of Tartu a free permit (non-exclusive licence) to reproduce, for the purpose of preservation, including for adding to the DSpace digital archives until the expiry of the term of copyright, my thesis

Radially anisotropic wormholes in $f(R,T)$ gravity,

supervised by João Luís Rosa, PhD.

2. I grant the University of Tartu a permit to make the thesis specified in point 1 available to the public via the web environment of the University of Tartu, including via the DSpace digital archives, under the Creative Commons licence CC BY NC ND 4.0, which allows, by giving appropriate credit to the author, to reproduce, distribute the work and communicate it to the public, and prohibits the creation of derivative works and any commercial use of the work until the expiry of the term of copyright.
3. I am aware of the fact that the author retains the rights specified in points 1 and 2.
4. I confirm that granting the non-exclusive licence does not infringe other persons' intellectual property rights or rights arising from the personal data protection legislation.

Paul Martin Kull

25.05.2022